Chemical Geology 439 (2016) 189–204

Contents lists available at ScienceDirect

Chemical Geology

journal homepage: www.elsevier.com/locate/chemgeo

Extracting foraminiferal seawater Nd isotope signatures from bulk deep sea sediment by chemical leaching

Patrick Blaser [a,*], Jörg Lippold [b], Marcus Gutjahr [c], Norbert Frank [a,d], Jasmin M. Link [a,d], Martin Frank [c]

[a] Institute of Environmental Physics, Heidelberg University, 69120 Heidelberg, Germany
[b] Institute of Geological Sciences and Oeschger Centre for Climate Change Research, University of Bern, 3012 Bern, Switzerland
[c] GEOMAR Helmholtz Centre for Ocean Research Kiel, 24148 Kiel, Germany
[d] Institute of Earth Sciences, Heidelberg University, 69120 Heidelberg, Germany

ARTICLE INFO

Article history:
Received 18 March 2016
Received in revised form 23 June 2016
Accepted 25 June 2016
Available online 27 June 2016

Keywords:
Neodymium isotopes
Deep sea sediments
Early diagenesis
Ferromanganese oxyhydroxides
Palaeoceanography
Rare earth elements
Leaching

ABSTRACT

The seawater radiogenic neodymium ($^{143}Nd/^{144}Nd$) isotope signature is an invaluable tool for the reconstruction of past deep water provenance. Sedimentary foraminifera or fish teeth are among the most reliable archives known for Nd isotope based reconstructions of past seawater. As the distribution and preservation of these archives are limited, the extraction of hydrogenetic ferromanganese oxyhydroxides from bulk sediments provide an easily applicable alternative. This method, however, implies the risk of generating artefacts due to the possible release of non-seawater derived Nd during the extraction procedure. Here we revisit and further investigate the reliability of the extraction of seawater derived Nd isotope signatures via leaching of bulk deep sea sediments with two commonly used buffered acetic acid and acid-reductive mix solutions. Repeated application of such stepwise leaching procedures to different non-decarbonated sediments from distinct settings across the deep Atlantic Ocean shows pronounced elemental and Nd isotope trends during the leaching process in the laboratory. Our results show that seawater Nd isotope compositions are extracted together with carbonates and manganese oxides only at the beginning of the leaching series. During chemical extraction, the carbonates effectively work as a buffer preventing acid-induced mobilisation of Fe oxides and volcanogenic material. Once this buffer is consumed, potentially present volcanogenic phases are considerably attacked, leading to shifts in the extracted Nd isotope signal of up to +12 epsilon units. Such volcanogenic phases are a significant source of contaminant Nd reflected by markedly elevated Al/Nd signatures. We consequently propose a revised weak leaching protocol for carbonate bearing deep sea sediments, which is simple to use, provides excellent agreement with data obtained from uncleaned foraminifera, and can be easily screened for contamination.

1. Introduction

Over the last decade sedimentary bottom water derived neodymium (Nd) isotopes were established as a standard palaeoceanographic proxy for deep ocean circulation. Neodymium is one of the rare earth elements (REE) and as such delivered to the oceans via erosion from the continents (Frank, 2002; Goldstein and Hemming, 2003) or sediment-bottom water interaction along marine continental margins (Lacan and Jeandel, 2005a; Lacan et al., 2012; Wilson et al., 2012). Radiogenic ^{143}Nd is produced by the decay of ^{147}Sm and crustal $^{143}Nd/^{144}Nd$ signatures therefore depend on the age and Sm/Nd ratio of the rocks. Consequently, the continental Nd isotope signatures are imprinted onto ocean waters, and potentially altered by changes of erosional processes and weathering regimes (Öhlander et al., 2000; von Blanckenburg and Nägler, 2001). Once dissolved in the pelagic ocean, Nd has a mean residence time of 200 to 1000 years (Rempfer et al., 2011; Tachikawa et al., 2003) and is removed from seawater via particle scavenging. Since the major ocean basins exchange water on a comparable time scale, the distribution of dissolved Nd isotope compositions results from mixing of the major ocean water masses (Piepgras and Wasserburg, 1980; Piepgras et al., 1979). Although some questions remain regarding the Nd budget of the oceans (e.g. Rempfer et al., 2011), such as the role of boundary exchange (Carter et al., 2012; Lacan and Jeandel, 2005a; Rickli et al., 2014; Wilson et al., 2012) and biological cycling (Molina-Kescher et al., 2014a; Stichel et al., 2015; Zheng

* Corresponding author.
E-mail address: patrick.blaser@iup.uni-heidelberg.de (P. Blaser).

http://dx.doi.org/10.1016/j.chemgeo.2016.06.024
0009-2541/

et al., 2016), Nd isotopes have become a valuable and widely used provenance tracer of past water masses (Copard et al., 2010; Crocket et al., 2011; Pahnke et al., 2008; Piotrowski et al., 2004; Roberts et al., 2010; Skinner et al., 2013; Wilson et al., 2015).

1.1. Extracting bottom water Nd isotope signatures from deep sea sediments

Seawater derived Nd is mainly transferred into ocean sediments at or closely below the sediment-water interface (Lacan et al., 2012; Piepgras and Wasserburg, 1980; Tachikawa et al., 2003; van de Flierdt and Frank, 2010). In the past years, a wealth of different archives conserving a seawater derived Nd signal have been exploited for the reconstruction of past bottom water Nd isotope signatures. These include Fe-Mn crusts (e.g. Abouchami et al., 1999; Frank et al., 1999), cold water corals (e.g. van de Flierdt et al., 2006; Colin et al., 2010; Wilson et al., 2014), fish debris (e.g. Staudigel et al., 1985; Martin and Scher, 2004), reductively cleaned or uncleaned foraminifera (e.g. Vance and Burton, 1999; Klevenz et al., 2008; Roberts et al., 2010), and the dispersed hydrogenetic ferromanganese metal accretions on sediment particles (hereafter referred to as Fe-Mn oxyhydroxides, e.g. Rutberg et al., 2000; Piotrowski et al., 2004; Piotrowski et al., 2008; Crocket et al., 2011). All of these archives have inherent advantages and disadvantages, yet reconstructions of past ocean water Nd isotope signatures have been achieved with all of them. Ideally, foraminifera or fish fragments are manually picked from marine sediments for the most reliable and continuous reconstruction of deep water Nd isotope signatures on time scales of thousands of years (e.g. Roberts et al., 2012). However, while they are reliable, foraminifera or fish fragments are often not available in sufficient quantity for a hydrogenetic Nd isotope reconstruction of high precision and temporal resolution. Similarly, while deep sea corals allow for an excellent age control and high temporal resolution, they mainly thrive at mid-depths and continuous temporal coverage based on corals is often not achievable (Robinson et al., 2014). To fill these gaps, the usage of alternative archives is required. In this regard extracting the deep seawater derived Nd from hydrogenetic Fe-Mn oxyhydroxides of bulk sediments is the method of choice as it can be applied to a large variety of sediments (not restricted by the abundance of foraminifera or fish debris) and is less time consuming than foraminifera based reconstructions. However, several studies found that Nd isotope compositions extracted from bulk sediment Fe-Mn oxyhydroxides did not strictly reflect actual or reconstructed deep water signatures (Bayon et al., 2004; Elmore et al., 2011; Molina-Kescher et al., 2014b; Roberts et al., 2010; Wilson et al., 2013). In these cases, the local Nd isotope signatures extracted from the bulk sediments are thought to be contaminated by non-hydrogenetic sediment fractions in the laboratory and/or pre-formed Fe-Mn oxyhydroxides (Bayon et al., 2004; Kraft et al., 2013).

The commonly employed method for extracting seawater Nd bound to Fe-Mn oxyhydroxides in sediments by selective leaching of bulk sediment was successfully established in the 1960s (Chester and Hughes, 1967). Over recent years these methods have repeatedly been adapted, refined, and tested in order to optimise the extraction of hydrogenetic Nd incorporated into Fe-Mn hydroxides (e.g. Rutberg et al., 2000; Bayon et al., 2002; Piotrowski et al., 2004; Gutjahr et al., 2007). The most reliable results (based on comparison with seawater data and extractions from other archives) were achieved with an acid-reductive leach solution after the complete removal of carbonates from the bulk sediment using weak acetic acid. It is, however, challenging to extract Nd bearing Fe-Mn oxyhydroxides from sediments without releasing any Nd from the detrital fraction.

Recently, Elmore et al. (2011) and Wilson et al. (2013) identified the most likely sources of potential contamination in sediment leaches. Elmore et al. (2011) showed a systematic offset of Nd isotope signatures extracted from bulk sediments by acid-reductive leaching to those extracted from foraminifera in core top sediments of the North Atlantic. In their study, foraminifera Nd isotope signatures were in overall agreement with those from ambient deep water, whereas sediment leaches were significantly offset towards more radiogenic compositions in the vicinity of Iceland. The authors concluded that the application of the leaching technique must have released contaminant Nd from Iceland derived volcanogenic minerals, whereas the foraminifera were mechanically cleaned from such contaminants. Wilson et al. (2013) systematically investigated the effect of leaching exposure time and sample size based on sediments from the Mascarene Basin in the Indian Ocean. They showed that a radiogenic sediment component altered the hydrogenetic Nd isotope signature extracted from Fe-Mn oxyhydroxide phases. Notably, the authors observed that the degree of contamination was reduced when the preceding carbonate removal was weakened. Similar observations were also made by Molina-Kescher et al. (2014b), who were able to leach Nd isotope signatures closer to the overlying seawater when they did not decarbonate their core top sediment beforehand.

Before assessing the origins of Nd extracted with bulk sediment leaches, it is fundamental to understand the distribution of Nd in sedimentary foraminifera. Roberts et al. (2012) and Tachikawa et al. (2013) investigated foraminifera tests by laser ablation and microprobe analyses, respectively. They presented striking evidence that foraminiferal Nd is mostly concentrated in microscopic iron and manganese mineral phases on foraminiferal test surfaces and in between individual calcite layers within the tests. These Fe and Mn minerals must have formed after burial of the tests during early diagenesis. Their results indicated that the tests are much more pervaded by these hydrogenetic Fe-Mn phases than previously thought. The fact that the Nd concentration in the calcite lattice itself is orders of magnitude lower than in Fe-Mn oxyhydroxides (e.g. Martínez-Botí et al., 2009 and references therein) paired with insufficient removal of hydrogenetic mineral deposits from the calcite tests explains the variable success of retrieving the Nd isotope composition of surface waters from sedimentary planktonic foraminifera (Kraft et al., 2013; Roberts et al., 2012). This is also the reason why the Nd isotope signatures of cleaned and uncleaned foraminifera are often indistinguishable from each other (e.g. Elmore et al., 2011; Kraft et al., 2013) with only very few exceptions (e.g. Vance et al., 2004). Thus, even after reductive cleaning, in most cases deep water derived Nd hosted in residual Fe-Mn oxyhydroxides still dominates the extracted Nd isotope signal (Kraft et al., 2013; Piotrowski et al., 2012; Roberts et al., 2012).

1.2. Nd bearing sediment fractions

Deep sea sediments comprise multiple components, which are intrinsically diverse in terms of their formation, origin, their chemical properties, and their Nd isotope compositions. The most important criterion for their differentiation with respect to this study is whether or not Nd bearing phases are authigenic/hydrogenetic in nature. A conceptual view of different components of deep sea sediments is illustrated in Fig. 1. It is important to note that each individual component itself can be heterogeneous both in its chemical

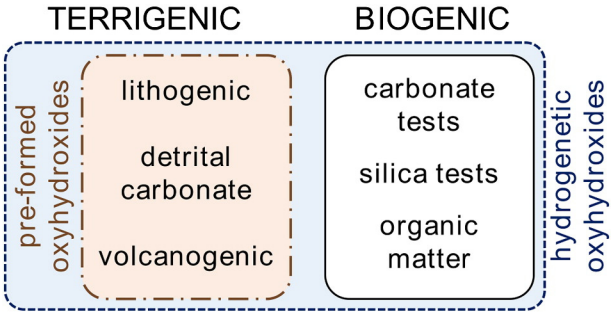

Fig. 1. Conceptual view of Nd bearing phases in deep sea sediments.

properties and in its Nd isotope signature. For instance, the composition of terrigenous material is dependent on the source area and the composition of hydrogenetic Fe-Mn oxyhydroxides depends on the environment from which they precipitated (e.g. Takematsu et al., 1989; Bau et al., 1996). The composition of foraminiferal calcite tests varies in trace metal concentrations and exact chemical properties from species to species, but also within individual tests, which must be taken into account when analysing incompletely dissolved foraminifera tests or bulk sediment leaches (Hathorne et al., 2003; Nürnberg et al., 1996). Furthermore, individual particles are readily separable under the microscope, whereas Fe-Mn oxyhydroxides can be deposited on the surface and in small cavities of any particle. Therefore, these different phases can only be effectively separated by selective chemical extraction.

During bulk sediment leaching, the applied reagents are inevitably in contact with both hydrogenetic and non-hydrogenetic sediment components, implying a potential source of contamination of the target hydrogenetic phase. The effect of contamination from non-hydrogenetic phases needs to be reduced to a minimum so that the extracted Nd isotope signature is identical to that of ambient bottom waters at the time of deposition, as well as to that of picked foraminifera from the same sediment. The terrigenous components presented in Fig. 1 inherently carry a non-authigenic Nd isotope signature and sometimes preformed Fe-Mn oxyhydroxides, which are also not derived from contemporary ambient seawater and thus present a possible source of contamination. Such phases were not observed in this study but have been described by Bayon et al. (2004); Kurzweil et al. (2010); Crocket et al. (2012), and Kraft et al. (2013). While the biogenic components all incorporate seawater derived Nd, not all of it originates from deep or bottom waters. Freslon et al. (2014) investigated the Nd content of sedimentary organic matter and found it to contain significant amounts of Nd incorporated in surface waters during growth. However, pelagic sediments commonly contain little residual organic matter and its Nd contribution to the bulk sediment can be expected to be low (Freslon et al., 2014; Martínez-Botí et al., 2009). Therefore, this component will not be further discussed in our study. Both biogenic carbonate and silica test lattices contain a Nd isotope signature sourced from their habitat (such as surface waters), but their respective Nd concentrations are comparatively low (see e.g. Tachikawa et al. (2014) for a review on foraminifera tests). All particulate components of deep sea sediments can be coated with hydrogenetic (Fe-Mn) oxyhydroxides, which are commonly enriched in trace metals. They are an ubiquitous, important sink for REE and thus clearly represent a valuable sedimentary archive for the reconstruction of past bottom water Nd isotope compositions if reliably extractable (Elderfield and Greaves, 1982).

In the following, we present the systematic gradual extraction of Nd and other elements from sediments during successive leaching. We are able to identify different Nd sources, their influence on the characteristics of the extracted solutions, and artefacts that can be introduced with different leaching approaches. Finally, we propose a refined and well constrained method for the extraction of hydrogenetic Nd from bulk sediments. This method yields Nd isotope compositions matching those of foraminifera even in regions where volcanogenic material used to prohibit the use of leaching techniques.

2. Materials and methods

2.1. Core sites and samples

A total of 19 sediment samples including one full procedural replicate from 11 different deep pelagic sites across the Atlantic Ocean were investigated (Table 1 and Fig. 2). Two different leaches were applied repeatedly to these samples in order to evaluate the (in)consistency of the extracted Nd isotope signal with ambient seawater. From each site, one sample near the core top of the sediment core (hereafter referred to as 'CT') was chosen to represent "quasi-modern" samples. Although they may not exactly be recent sediments, the sedimentological data and age models imply that they all represent the late Holocene. Reconstructed deep Atlantic pelagic seawater Nd isotope signatures of this time interval show little to no deviation from present-day seawater values (e.g. Gutjahr et al., 2008; Roberts et al., 2010; Lippold et al., 2016). Additionally, five samples from sediment layers deposited at approximately 130 ka before present (during glacial termination 2, 'TII' serve as examples of older sediment layers which may have undergone diagenetic maturation processes (Poulton et al., 2004) different from those affecting the core top material. These 16 sediments were obtained from water depths between 2769 m and 4584 m and from core depths between 1 cm and 32.25 m. They contain between 4 and 83 wt% carbonate and are referred to as 'ordinary'. For easier reference, the eleven sites are numbered from North to South in ascending order (Fig. 2 and Table 1).

Two compositionally distinct samples from site 7 representing an ice rafted debris (IRD) layer deposited during Heinrich Stadial 1 and an Icelandic ash turbidite sample (ASH) deposited during the early Holocene were also included to represent extreme depositional environments. Jantschik (1991) described North-East Atlantic core Me-68-91 (site 7,

Table 1
Sediment samples processed following our progressive leaching protocols.

Site #	Core	Lat. [°N]	Long. [°E]	Water depth [m]	Sample depth [mcd]	$CaCO_3$[a] [%]	Sample label	Age model
1	ODP 643	67.72	1.03	2769	0	51	CT	Henrich and Baumann (1994)
					3.98	5	TII	
2	IODP 1305	57.48	−48.53	3459	0	32	CT	Hillaire-Marcel et al. (2011)
					32.25	4	TII	
3	IODP 1314	56.36	−27.89	2799	0	48	CT	Alvarez Zarikian et al. (2009)
					12.5	10	TII	
4	IODP 1304	53.06	−33.53	3065	0.03	49	CT	
5	IODP 1302	50.17	−45.64	3556	0	38	CT	Hillaire-Marcel et al. (2011)
6	IODP 1308	49.88	−24.24	3873	0.02	70	CT	Hodell et al. (2008)
7	ME-68-91 VL	47.43	−19.58	4470	0	75	CT[b]	
					0.33	25	ASH	Jantschik (1991)
7	ME-68-91 HL	47.43	−19.58	4470	0.51	34	IRD	
8	IODP 1313	41.00	−32.96	3413	0	78	CT	Stein et al. (2009)
9	ODP 1063	33.69	−57.62	4584	0.105	29	CT	Böhm et al. (2015)
10	ODP 659	18.08	−21.03	3071	0	58	CT	Kuechler et al. (2013)
					4.20	21	TII	
11	ODP 1267	−28.10	1.71	4354	0	83	CT	Bowles (2006)
					1.12	32	TII	

Notes:
[a] $CaCO_3$ content estimated by assigning total amount of Ca extracted by 10 Ac-leaches to $CaCO_3$.
[b] Sample 7 CT was completely replicated once.

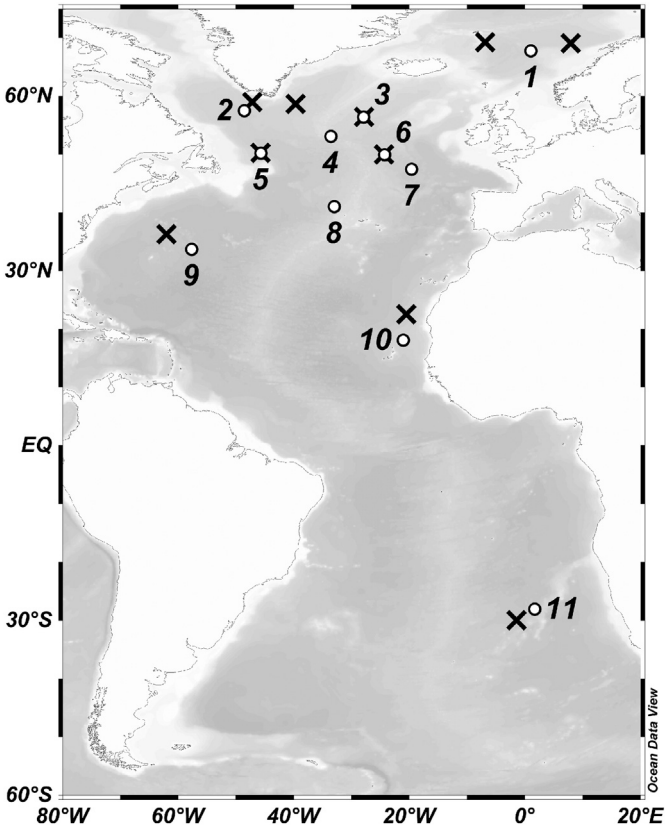

Fig. 2. Sites of investigated sediment cores (open circles) and nearby locations of existing seawater Nd isotope data (black crosses, Lacan et al., 2012; Frank et al., 2014; Lambelet et al., 2016). The core sites are labelled in ascending order from North to South for easier reference in the text. See Table 1 for locations and sample descriptions.

Table 1) in detail and found that the grain size of the IRD layer is dominated by the sand fraction and contains a high percentage of newly formed hydrogenetic dolomite and virtually no foraminifera. Therefore, this IRD sample is representative of extreme sediment composition and pronounced sediment alteration. Sample 7 ASH is dominated by volcanogenic material and is considered an end member for volcanogenic contributions to North Atlantic marine sediments. We refer to these two samples as 'extraordinary' and exclude them from assessments of the average composition of the leachates (i.e. extracted leaching solutions), unless stated otherwise.

In order to compare the leached Nd isotope signatures to the seawater signatures extracted from Fe-Mn oxyhydroxides of planktonic foraminifera, tests of the >63 μm size fractions were hand-picked either from the same sediment or, if not enough material was available, from within ±2 cm of the original layer. The only exceptions are samples 7 CT and ASH. To exclude potential contamination of the sediment near the ash layer we used core top and mid-Holocene foraminifera samples from a nearby core (Me-69-196 VL, 1 and 9 cm depth) as uncontaminated references.

2.2. Sample treatment

2.2.1. Sediment handling

For the determination of foraminiferal Nd isotope signatures, tests were picked from the coarse (>63 μm) fractions of sieved bulk sediment samples and prepared following the procedure described in the review by Tachikawa et al. (2014). This method includes mechanical separation of the tests from particles and subsequent dissolution (without removing any Fe-Mn oxyhydroxides beforehand) by slow addition of acetic acid and remaining residue was discarded.

In several previous studies deep water Nd isotope signatures were obtained from the dispersed hydrogenetic Fe-Mn oxyhydroxide fraction after complete removal of carbonates from the sediment (e.g. Bayon et al., 2004; Piotrowski et al., 2004; Gutjahr et al., 2007; Martin et al., 2010; Elmore et al., 2011; Wilson et al., 2013; Molina-Kescher et al., 2014b; Böhm et al., 2015). These authors used (in some instances buffered) acetic acid for the decarbonation of the sediment before extracting the Nd bearing metal oxyhydroxides with an acid-reductive solution containing hydroxylamine hydrochloride as a key reagent. It is important to note, however, that many of the chemical protocols used for these selective leaching procedures differed from each other in reagent concentrations, duration of the application or sample to solution ratios. Here we refer to such leaching methods with prior decarbonation as 'conventional leaches'. To obtain new insights into the processes taking place during the leaching procedures we repeatedly applied one acetic acid solution and one acid-reductive solution to the same sediment samples. The two solutions employed were a buffer solution of acetic acid and Na-acetate in a ratio of 1:1 at 0.1 M (pH = 4.6, abbreviated as "Ac" hereafter) and a mixture of 1.5% (0.26 M) acetic acid, 0.005 M hydroxylamine hydrochloride, and 0.003 M Na-EDTA, buffered to a pH of 4 using NaOH (abbreviated as "HH"). These two leaching solutions represent dilutions of those used in Gutjahr et al. (2007). The dilution factors are approximately 5 and 10, respectively. It is important to note, however, that due to the overall larger solution volume used in this study and the repeated replacement of the solutions they are likely to have a stronger leaching effect than their concentrated counterparts applied only once. This diluted HH-leach is also very similar to the ones used by Haley et al. (2008) and Chen et al. (2012) for carbonate-free Arctic sediments. An overview of the leaching experiments presented in this work is illustrated in Fig. 3. The bulk sediment samples were freeze-dried and manually ground for homogenisation. Two splits of 0.25 to 0.3 g of sediment were washed for about 30 min with ultra pure water (18.2 MΩ) on a vertical tube rotator wheel and then subjected to ten successive leaches with either the Ac or the HH solution, respectively. Every single leaching step comprised the addition of 10 ml of the respective leaching agent to the sample in a 15 ml centrifuge tube. After degassing, the samples were placed on the vertical tube rotator and left to rotate for one hour at room temperature. Hereafter, the vials were centrifuged at 4000 rpm for 10 to 40 min until complete settlement of the suspended sediment particles was achieved. The solutions were carefully decanted and prepared for element concentration measurements and chemical separation of the Nd fraction. The sediment residue was washed with ultra pure water and centrifuged so that the water could be discarded before the repeated addition of 10 ml leaching solution. At the start of both, the washing and the leaching steps, the samples were thoroughly suspended manually and

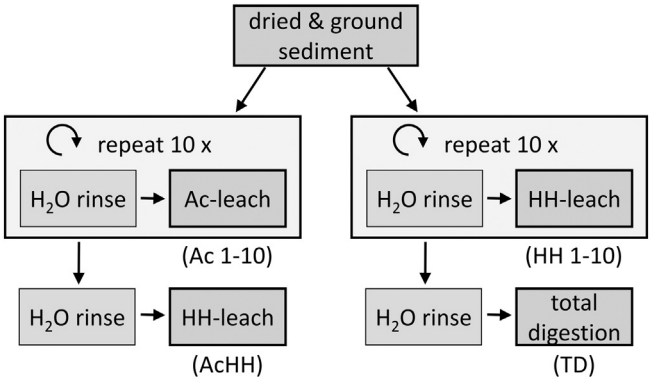

Fig. 3. Schematic view of the applied sediment treatments (leaches, rinses, total digestions) and their order. Two splits of each sediment were analysed independently from each other with 10 repetitions of either Ac or HH-leaches. The samples were rinsed once with ultra pure H_2O between successive treatments. Sample names used in the text are given in parentheses.

with a vortex shaker until the sediment was well dispersed. However, occasionally, some small agglomerations remained visibly stuck together. The results of these successive leaching steps are termed Ac-leaches 1 to 10 and HH-leaches 1 to 10, respectively.

After the 10th Ac-leach step the sediment residues of the core top and the extraordinary samples were treated with a final HH-leach for comparison. We call this step the AcHH-leach. AcHH-leaches are similar to the conventional leaching methods, because the carbonates had been completely removed before the HH-leach, albeit excess acetic acid buffer has been used and the HH-leach applied is weaker than in most other conventional methods. The sediment residues of the core top and the extraordinary samples after the 10th HH-leach were completely digested in a microwave oven using a mixture of concentrated HF, HCl, and HNO_3 in order to determine the elemental compositions and the Nd isotope signatures of the detrital sediment fractions (total digestions, TD). Drying of the total digestion solutions lead to the formation of insoluble particles in some cases, most likely calcium fluorides (Yokoyama et al., 1999). Parallel analysis of several reference materials showed that this significantly reduced the concentrations of some elements in the analytes, most importantly of Ca. Thus, the Ca contents (and Si, which degases as SiF_4, see e.g. Croudace, 1981) of the total digestions cannot be interpreted quantitatively. The contents of other elements may also be reduced due to co-precipitation with insoluble particles but deviations from the literature values in the reference materials were always below 20%.

Additionally, we carried out a simple experiment on the dynamics of the pH evolution in the leaching solution and its dependency on the carbonate content in the sediment. The details of this pH experiment can be found in the supplementary material S.4.

The applied hydrofluoric acid, Na-EDTA, and hydroxylamine hydrochloride were of pA quality, distributed from Merck. All other chemicals were used in 'supra pure' quality (Merck, or comparable from VWR in the case of HCl and HNO_3) to assure low background contaminations.

2.2.2. Chemical preparation and measurements

Extracted solutions were evaporated to dryness, re-dissolved in 1 ml concentrated HNO_3, and evaporated again. This step was repeated and a few drops of 25% H_2O_2 were added to decompose any remaining organic material. Following re-dissolution in 7 M nitric acid, an aliquot was separated for concentration measurements. The remaining sample was dried down and re-dissolved in the acid required for the subsequent column chemistry, if Nd isotope compositions were to be measured.

Separation of the Nd fraction was carried out applying standard techniques (Cohen et al., 1988). Rare earth elements were first separated from the bulk sample by cation exchange chromatography using 50W-X8 (200–400 mesh) resin. The Nd fraction was further isolated from the other light REE using Ln-spec resin (100–150 μm, Pin et al., 1994).

Nd isotope measurements were carried out on a Nu Instruments MC-ICP-MS at GEOMAR in Kiel. Instrument-induced mass fractionation was corrected to a $^{146}Nd/^{144}Nd$ value of 0.7219 using an exponential law. The corrected $^{143}Nd/^{144}Nd$ ratios were then normalised to the accepted value of 0.512115 based on repeatedly measured JNdi-1 standard solutions (Tanaka et al., 2000). Nd isotope signatures are reported as $\varepsilon_{Nd} = ([(^{143}Nd/^{144}Nd)_{sample} / (^{143}Nd/^{144}Nd)_{CHUR}] - 1) * 10{,}000$, where $(^{143}Nd/^{144}Nd)_{CHUR} = 0.512638$ denotes the "Chondritic Uniform Reservoir" (Jacobsen and Wasserburg, 1980). The reproducibility for different sessions based on repeated measurements of the JNdi-1 standard and dedicated samples varied between 0.22 and 0.43 ε_{Nd} units (2 standard deviations), with the exception of one run with foraminifera samples at low concentrations, resulting in a reproducibility of only 0.76 ε_{Nd}.

Elemental compositions were measured with a Thermo Fisher iCap ICP-QMS in combination with an Elemental Scientific Apex desolvator at the Institute of Environmental Physics at Heidelberg University. The samples were measured at two different concentrations. Ca was kept below 5 ppm in order to avoid significant matrix effects. Since large amounts of Na were contained in the leaching solutions, its concentrations could not always be kept similarly low. Thus, some measurements were conducted at Na concentrations of up to 29 ppm with calibration standards (mixed from single-element standards from Inorganic Ventures) adjusted to this higher Na matrix. Measured intensities were corrected for isobaric interferences. The oxide formation of Ba and the REE were monitored using mixed control solutions (containing Ba, Ce, Tb, Ho, and Tm) during the measurement sequences. Molecular interferences on Eu and Gd were thus corrected for. For most samples, the major elements were additionally measured on an Agilent ICP-OES 720 at the Institute of Earth Sciences at Heidelberg University in order to cross-validate the results obtained by ICP-QMS (especially for Al and Fe, which suffer under a high background intensity on the ICP-QMS). For all concentration measurements acid blanks were subtracted and the inherent instrument drift was monitored and corrected by measuring in-house mixed multi element solutions (Inorganic Ventures) of known concentrations every 6th to 12th sample. Blank contributions from the leaching solutions were measured and found to be overall insignificant. Typical precision of the concentration measurements was better than 10% (2 standard errors), which is very small in view of the observed variability of the samples of several orders of magnitude. Concentrations in the leachates are given as μg per g of dried bulk sediment of the original sample prior to leaching. Hence, these "concentrations" rather reflect the amount of the respective element leached than its weight fraction in the leached material given that the total mass of the latter is not precisely known. REE were normalised to Post Archaean Australian Shale (PAAS, Nance and Taylor, 1976) in order to evaluate the REE patterns as given in Martin et al. (2010). The parameters to characterise these patterns are accordingly defined as:

$$\text{Cerium anomaly}: \quad Ce/Ce* = [Ce]/\overline{[La],[Pr]}; \tag{1}$$

$$\text{Europium anomaly}: \quad Eu/Eu* = [Eu]/\overline{[Sm],[Gd]}; \tag{2}$$

$$\text{Light REE}: \quad LREE = \overline{[La],[Pr],[Nd]}; \tag{3}$$

$$\text{Middle REE}: \quad MREE = \overline{[Gd],[Tb],[Dy]}; \tag{4}$$

$$\text{Heavy REE}: \quad HREE = \overline{[Tm],[Yb],[Lu]}; \tag{5}$$

$$\text{REE slope}: \quad HREE/LREE \tag{6}$$

$$\text{REE bulge}: \quad MREE/MREE* = MREE/\overline{LREE,HREE} \tag{7}$$

3. Results

3.1. Elemental concentrations

The elemental composition of the leachates varied largely in both abundance and in relative change of the concentrations during progressive leaching. They cannot be described in all detail here and we focus on general trends and distinctive features across the different samples. As an example the evolutions of the most important major and trace element concentrations during both leaching series are shown for the three samples of site 7 in Fig. 4. The complete data set is provided in supplementary material S.1, the discussed elemental ratios are plotted in S.2, and selected REE distributions in S.3. The range of elemental abundances across all ordinary samples is given in the box-and-whisker plot in Fig. 5. Due to the comparable chemical behaviour of individual REE, their variation in concentration is also similar. Therefore, Nd was chosen to represent REE concentrations, whereas the shapes of the REE patterns are parameterised by the REE ratios described in Eqs. (1) to (7).

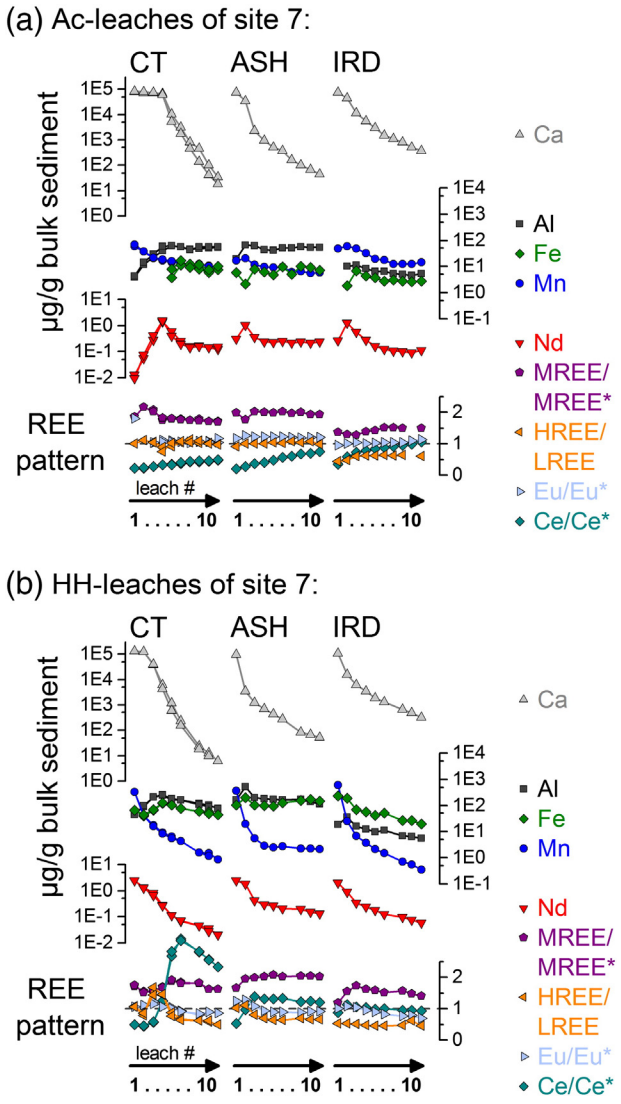

Fig. 4. Typical trends in selected element concentrations and REE ratios in the leachates extracted during the progressive Ac-leaching (a) and HH-leaching (b) sequences. All three samples displayed are taken from site 7. The core top sample shows element concentration patterns during the successive leaching similar to the other carbonate-rich samples investigated in this study (cf. S.1). The integrity of our data is demonstrated by a full procedural replicate of the core top sample in (a) and (b). The six panels in (a) and (b) show the major and trace element data from progressive leaching steps 1 to 10. Note the logarithmic y-axes for the concentration data.

As expected, Ca, Sr, and Mn exhibit their highest concentrations at the beginning of both leaching procedures and decrease monotonically by orders of magnitude during the subsequent leaching steps (Figs. 4 and 5 and Table S.1). This decrease occurs significantly earlier in the course of the HH-leaching steps. In contrast, Al, Nd, and Fe behave very differently. In most cases, Al is initially depleted, but reaches a persistently high level when Ca concentrations begin to decline. A similar trend with a very sharp peak is observed for the Nd content in the Ac-leaches (cf. Fig. 4 and S.1), whereas the Nd concentrations in the HH-leaches resemble the trends of Ca and Mn. Changes of the Fe concentrations depend more on the individual sample and vary between Mn-like and Al-like behaviour. In several HH-leaching sequences Fe shows a small decreasing trend from the first to the second or third leach, after which they increase similarly to Al (cf. Fig. 4 and S.1). Ce is generally depleted ($Ce/Ce^* \approx 0.4$ to 0.5 in average) at the beginning of the leaching and exhibits an increasing tendency during further leaching steps. In the HH-leach sequences it becomes enriched (up to $Ce/Ce^* \approx 12$ for samples from site 11, and up to 1.5 to 4 for the other samples) before approaching 1 again at the end of the sequence for most samples. Exceptions are the HH-leaches of 4 out of 5 TII samples (sites 1, 2, 3, and 10) and sample 7 IRD, where the Ce anomaly remains nearly constant and rather small. The europium anomaly of the Ac-leaches remains relatively constant and slightly elevated in the course of the progressive leaching with values ranging between 1 and 1.2, similar to the foraminifera samples. Notable exceptions are the first or second Ac-leaches of samples 6, 7, 9, and 11. The REE concentrations in these leaches, however, are very low and thus this effect might be a measurement bias. During the progressive HH-leaches, Eu/Eu* undergoes a smooth transition from values similar to those in the Ac-leaches towards depleted values (as low as 0.76 in sample 2 TII) and in some cases upwards again. The europium anomaly in the total digestions varies between 1 and 1.5, with more pronounced anomalies for the northern North Atlantic samples and sample 7 ASH (Fig. 5, S.2 and S.3). The slope of the REE pattern and the mid REE enrichment both show a complex behaviour. MREE/MREE* are generally high with values between ~1 and 2.5 (across all samples and leaches). Most of the variation in the leaching series of the individual samples occurs during the first four leaches and both increases and decreases are observed, depending on the type of sediment (S.1 and S.2). Afterwards, MREE/MREE* are levelled between 1.5 and 2.2 in the Ac-leaches and tend to slightly lower values in the HH-leach series. Heavy REE can become both enriched or depleted in the course of the individual leaching series and also show highest variability in the first leaches, whereas towards the end of the sequence they are usually depleted or equal to the light REE (HREE/LREE = 1).

Ca and Sr concentrations initially remain constant and elevated up to the 4th Ac-leach or the 3rd HH-leach, depending on the carbonate content of the sample. Thereafter, the concentrations drop by several orders of magnitude. Together, these initial leaches contain up to 60% and 97% of the total leached Nd. Interestingly, the amount of Nd extracted with the first HH-leach is remarkably consistent across the 16 ordinary sediments, with concentrations ranging from 2 to 5 µg per g bulk sediment used. The Nd concentrations in the REE-peaks of the Ac-leaches (cf. Fig. 4 and S.1) are less homogeneous and generally lower. Between 27% and 89% of the total Nd contained in the sediment (assessed by the sum of all HH-leaches plus the TD) are leachable and removed with 10 HH-leaches. In comparison, Ac-leaches release significantly less Nd (5%–59% of the total Nd) from the same sediment samples. In the case of Mn, Al, and Fe the ten HH-leaches extracted up to 99%, 20%, and 16% of the total content of the bulk sediment, with mean values of 84%, 8%, and 9%, respectively. In contrast, the Ac solution only extracted about 19%, 2%, and 0.4% in average of the total content of these three metals, respectively.

3.2. Neodymium isotope signatures

All Nd isotope data measured in this study are displayed in Fig. 6 together with data obtained from foraminifera and conventional reductive leaches of core top sediments from nearby locations previously published by Elmore et al. (2011). The sediment data is complemented by nearby Nd isotope measurements of deep waters (Frank et al., 2014; Jeandel, 1993; Lacan and Jeandel, 2005a, 2005b, 2004a, 2004b; Lambelet et al., 2016; Piepgras and Wasserburg, 1983; Tachikawa et al., 1999). Since the amount of Nd extracted was low in the first Ac-leaches and the later steps of Ac- and HH-leaches (Figs. 4 and 5), we could not obtain Nd isotope data for all leaching steps. The results of the full procedural replicate of sample 7 CT (Fig. 6b, replicates) demonstrates excellent reproducibility. All replicate Nd isotope data reproduce within analytical uncertainty (even for the fourth successive HH-leach and fifth Ac-leach).

The first HH-leaches agree with compositions retrieved from uncleaned hand-picked planktonic foraminiferal tests of the same core and similar sediment depth (this study and Elmore et al., 2011) for all but one ordinary samples (Fig. 7). However, the initial HH-leaches and foraminifera samples both show distinct deviations from the local or

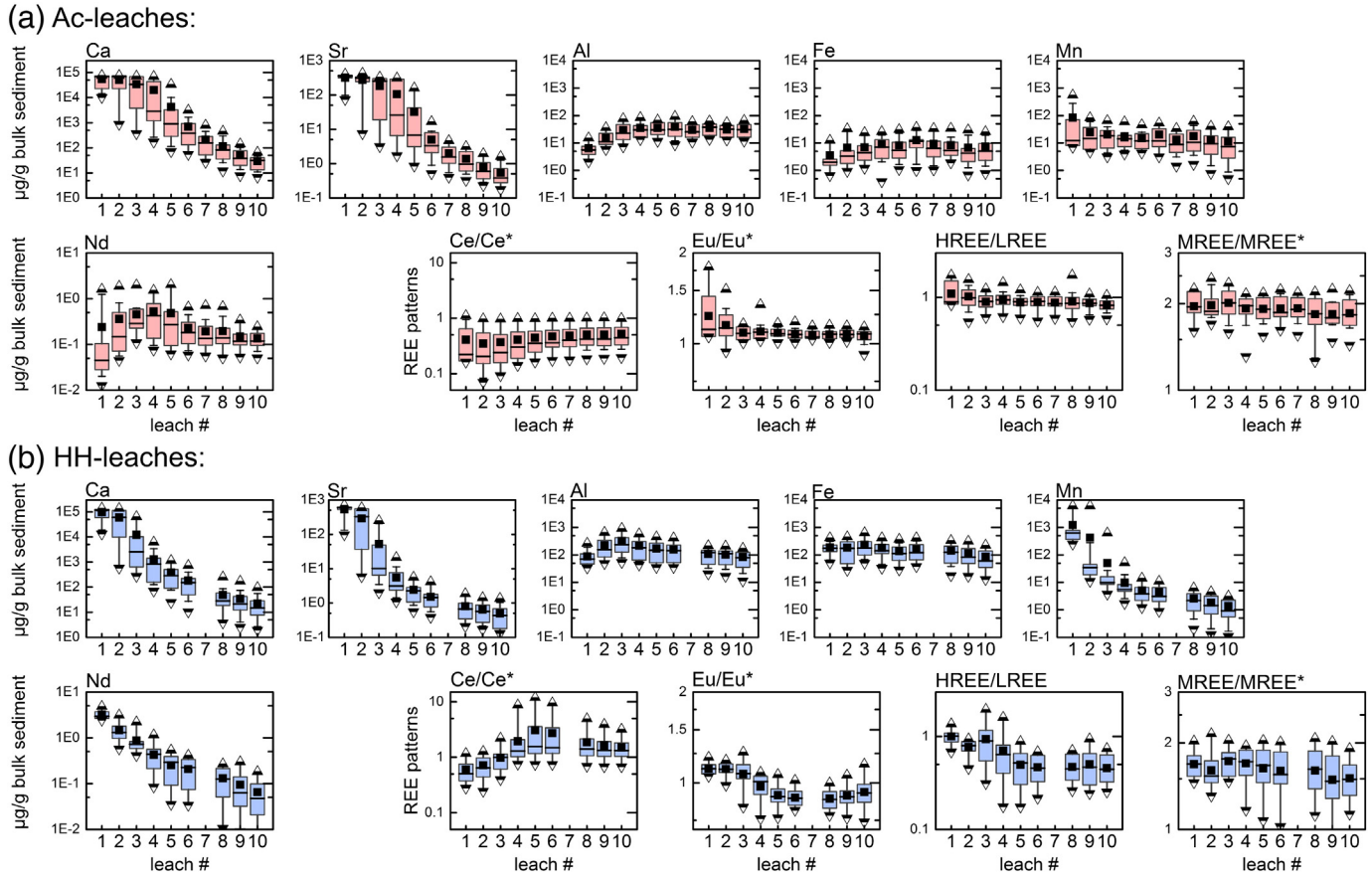

Fig. 5. Box-and-whisker plots of the statistical distribution of the major element concentrations and REE data of all investigated sediment samples (16 samples from 11 sites) except the ASH and IRD samples of site 7 (which are shown in Fig. 4). The black horizontal bar and square mark the median and mean values, respectively. 50% of the results lie inside the boxes and 80% in between the whiskers. The triangles span the complete range of the data. (a) Data for the 10 successive Ac-leaches. (b) Data for the 10 successive HH-leaches. HH-leaches #7 were lost during preparation. Note the different logarithmic y-axes for individual elements. Scales for (a) and (b) are equal.

regional deep seawater ε_{Nd} signatures in some cases. This is particularly the case in the northern North Atlantic in core top samples from sites 1 through 4 ($\Delta\varepsilon_{Nd} \approx 1.5$–2). Also, in each sample, the first measured signature of the Ac-leaches agrees within analytical uncertainty with the first HH-leach. Furthermore, the data clearly show that the Nd signatures extracted by the HH-leaches change systematically towards more radiogenic values during the progressive leaching procedure, in most cases until a stable offset towards more radiogenic values is reached. For samples from sites 1–4 and sample 7 ASH, this trend is particularly pronounced after the first to second leach spanning a range of up to 11.5 ε_{Nd} units. In samples 2 CT and possibly 3 and 4 CT, the extracted signatures show a reversed trend towards unradiogenic values after the radiogenic peak in the middle of the extraction sequence (Fig. 6). Initial Ac- and HH-leaches of the IRD sample both show the least radiogenic ε_{Nd} signature obtained during this study of −25.5, followed by a shift towards more radiogenic values over the course of the leaching series. The Ac-leach signatures of the ordinary samples vary significantly less than the HH-leaches; relevant trends towards more radiogenic values are only apparent in the TII sample from site 2 and the extraordinary samples. Nd isotope signatures of the AcHH-leaches from sites 1 through 4 CT and 7 ASH and IRD are offset by up to 5.8 ε_{Nd} units from the initial HH-leaches towards radiogenic isotope compositions, similar to the later HH-leaches. Only the AcHH-leach of sample 10 CT shows a signature that is closer to the nearby deep water measurements than the foraminiferal or HH-leach 1 isotope signatures. In 4 out of 6 cases the conventional leaches of Elmore et al. (2011) are significantly offset (between 4 and 11 ε_{Nd} units) from seawater and our first HH-leaches. This is especially the case for those sites where the progressive HH-leaches show large variations, but also in sample 8 CT from the central North Atlantic near the Azores. In the latter case, however, the sample used by Elmore et al. (2011) was taken from 15 cm deeper in the core than the one we used. The Nd isotope signatures of the digested residuals (TD) differ from the first HH-leaches in a range of +7 to −7 ε_{Nd} units and in no case match with these within their 2 standard deviations.

4. Discussion

4.1. Leached components and their reactivities

4.1.1. Carbonate dissolution

Both the Ac- and HH-leaches show high Ca concentrations in the first leaching steps, dominating the leachate composition. Assuming that all Ca originates from $CaCO_3$ and that it represents the bulk of the carbonates dissolved, the amount of extracted carbonate can be estimated. We find that the employed single 10 ml Ac-leaches dissolved up to 50 mg calcium carbonate (or 18% of the total sample mass) whereas the HH-leaches released about twice that amount from the sediment per leach. Due to the high $CaCO_3$ content in some of the samples, we thus find continuously high Ca concentrations in the Ac-leaches up to the fourth leach and the HH-leaches only up to the second (Fig. 5). Together with Ca, Sr exhibits a high linear correlation throughout both the Ac- and HH-leaching series ($R^2 = 0.95$ across all samples). Sr/Ca ratios of the first leaches vary between 3.9‰ and 14.3‰ (mass/mass) except for sample 7 IRD, which features much lower ratios of 1.3‰ and 1.0‰ in the first Ac and HH-leach, respectively. This observation is consistent with Jantschik (1991), who related low Sr/Ca values to the dissolution of authigenic calcium carbonate precipitates. Calcium carbonate thus

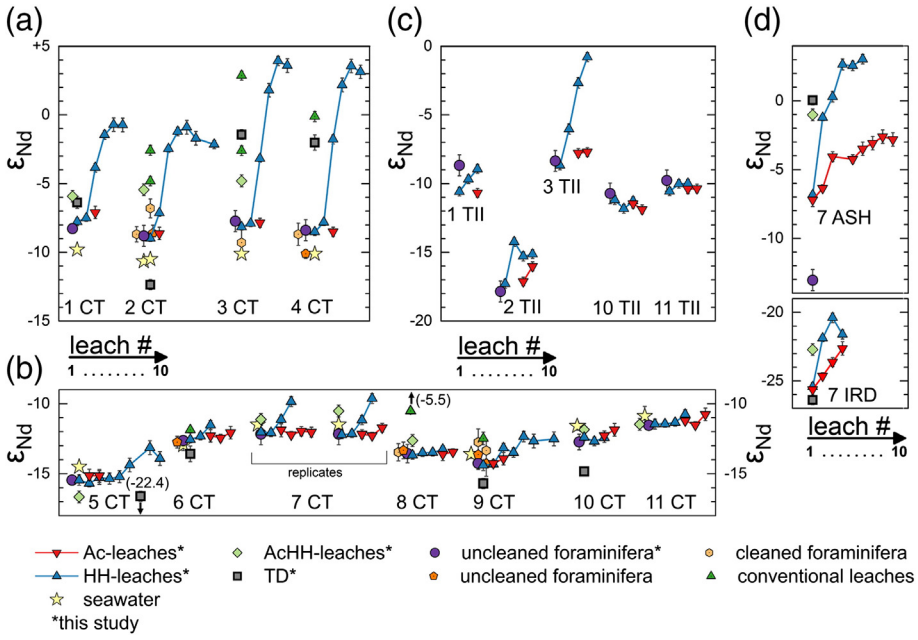

Fig. 6. Evolution of the Nd isotope signatures in the leachates, foraminifera, and total digestions in the studied sediment samples. The data comprise Ac-leaches (red downward triangles), HH-leaches (blue upward triangles), AcHH-leaches (green diamonds), total digestions of the residuals (black squares), and uncleaned foraminifera (purple circles) from this study. They are complemented by cleaned and uncleaned foraminifera (orange hexagons and pentagons, respectively) and conventional leach data (green upward triangles) from Elmore et al. (2011) and proximate deep water data from Piepgras and Wasserburg (1983); Jeandel (1993); Tachikawa et al. (1999); Lacan and Jeandel (2004a); Lacan and Jeandel (2004b); Lacan and Jeandel (2005a); Lacan and Jeandel (2005b); Frank et al. (2014); Lambelet et al. (2016). Numbers at the bottom of the panels refer to the different sites (see Table 1). Nd isotope signatures of the leaches are presented in ascending order of leaching steps from left to right for each individual site. (a): Northern North Atlantic sites, CT samples. (b): Sites with modest trends during leaching, CT samples. (c): TII samples. (d): Nd isotope signatures of the two extraordinary samples (ASH and IRD of site 7). Note that Nd concentrations are much lower in the Ac-leaches, especially in the initial ones, and thus the Nd isotope signature could only be determined for a few of these leaches. Error bars represent 2 σ external reproducibility. (For interpretation of the references to colour in this figure legend, the reader is referred to the web version of this article.)

represents the most reactive component in the sediments when exposed to acidic reagents (cf. Tessier et al., 1979; Bayon et al., 2002). This conclusion is supported by the results we obtained from the pH experiment (see supplementary material S.4). The carbonate fraction dominates the neutralisation reaction during the leaching process and thus the prevailing pH of the leach solution. Furthermore, the reaction of carbonate and acid proceeds rapidly (see S.4). We thus conclude that the effectiveness of the applied acids for the reaction with other phases is controlled by the calcium carbonate content of the sample at the start of the leaching (in addition to the initial pH and acid concentration of the leach solution itself). It is important to note that this is a major difference to conventional leaches, for which the carbonate is removed with a weak acid before the Fe-Mn oxyhydroxides are targeted with an acid-reductive leach.

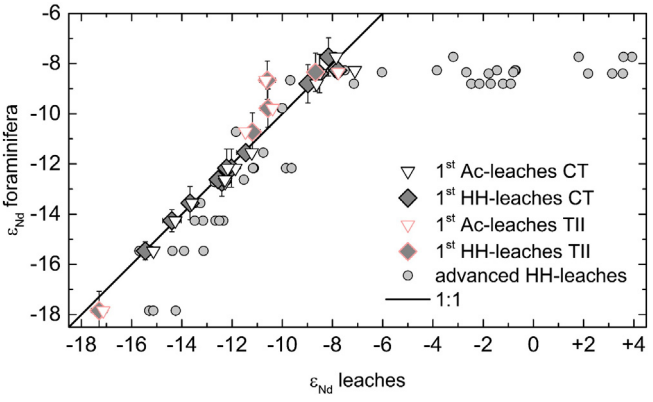

Fig. 7. Comparison between leached Nd isotope signatures (x-axis) from the ordinary samples with those from picked foraminifera (y-axis). Dark grey diamonds mark the 1st HH-leaches, small grey circles the signatures from all later HH-leaches. White downward triangles show the correlation of the first measured Ac-leaches in the sequence with the same foraminifera. Black lined symbols are CT samples and red lined symbols stand for TII samples. The black line delineates a 1:1 correlation between the Nd isotope signatures of the foraminifera and those of the leachates. Error bars are only shown for all 1st leaches when larger than the symbol size. (For interpretation of the references to colour in this figure legend, the reader is referred to the web version of this article.)

4.1.2. Hydrogenetic Fe-Mn oxyhydroxides

The fact that Mn and REE are released predominantly at the beginning of the HH-leaching sequence (Figs. 4 and 5) points to Mn (oxyhydr-)oxides being dissolved together with the carbonates. Although it might be expected that Fe-Mn oxyhydroxides dissolve uniformly, Fe concentrations are low in the first HH-leaching steps (and remain relatively constant) so that the Fe/Mn ratios of the first HH-leaches range from 0.03 to 0.7 across all samples (cf. S.2). In contrast, the Fe/Mn ratio in the AcHH-leaches varies between values as low as 5×10^{-4} and 1.9. The uncleaned foraminifera exhibit overall Fe/Mn ratios in a range from 0.03 to 1.9. The ratio of the total leached Fe and Mn over the course of the 10 HH-leaches and for the different samples spans a range between 0.2 and 4.4, with a mean value of 1.9. Gutjahr et al. (2007) and (2010) measured Fe/Mn ratios in their conventional sediment leaches in the northwest Atlantic ranging from 0.6 to 150 in the former and 0.33 to 0.75 in the latter work (Holocene to Last Glacial and MIS3 sediments, respectively). Previous studies found that ferrous compounds can be mobilised with buffered acetic acid, whereas an acidic HH-leach can dissolve the 'easily reducible' minerals such as ferrihydrite, lepidocrocite, and to a minor extent also akaganéite (Poulton and Canfield, 2005). Other Fe minerals like goethite and hematite were found to be resistant to these solutions. Interestingly, Mn oxides seem relatively resistant to buffered acetic acid solutions, but susceptive to solutions similar to our HH-leach (Chester and Hughes, 1967; Koschinsky and Halbach, 1995).

A possible explanation for the low Fe/Mn ratios in our initial Ac- and HH-leaches is that the dispersed hydrogenetic oxyhydroxides in these samples indeed mainly consist of Mn rather than Fe compounds. This

could mean that most of the Fe extracted later in the leaching sequence originates from lithic material and thus represents contamination by non-hydrogenetic sources. It seems unlikely, however, that the Fe-Mn oxyhydroxides in all our different samples are significantly depleted in Fe compared to Mn. Another possibility is that the extracted trace metals are indeed derived from a mixture of Mn- and Fe-oxyhydroxides, but the mobilisation of the latter depends much more on the pH of the leachate. As discussed above, the presence of carbonates rapidly buffers the acid in the leach solution and increases the pH quickly and significantly. Thus, as long as enough carbonate is present in the sediment, only little Fe is being mobilised. Following this line of reasoning, the Fe extracted later in the leaching sequence could actually partially or completely be hydrogenetic in origin (abovementioned easily reducible minerals), and the preferential dissolution of Mn over Fe leads to the low Fe/Mn values. The calculated Pourbaix diagrams (e.g. Takeno, 2005) of Mn and Fe in idealised dilute solutions seem to support this effect. Although our solutions are not as simple as in these calculations, it is conceivable that the relative behaviour of Mn and Fe remains similar, and thus the dissolution of Fe would indeed be more dependent on the pH than the dissolution of Mn. Note, however, that the REE abundances do not follow the Fe concentration patterns but rather show highest concentrations at the beginning of the HH-leach series, which implies that they are either predominantly bound to Mn-oxides or preferentially released from hydrogenetic Fe-Mn oxyhydroxides. In contrast to early observations (Chester and Hughes, 1967), our 10 Ac-leaches extracted relatively high amounts of Mn (between 4% and 85% with an average of 36% of the amount in the 10 HH-leaches), which may indicate that a relatively large fraction of the Mn is associated with carbonates or other less stable Mn mineral phases, as was similarly observed by Gourlan et al. (2010). However, this fraction is significantly smaller for the core top samples than for the older TII samples (averaging 15% and 70% of the amount released with 10 HH-leaches, respectively, at the five sites where both young and old samples were investigated). This may indicate a diagenetic effect, transforming the Mn bearing fraction into a more acid-soluble form. One possibility would be diagenetic formation of manganese carbonate (Boyle, 1983; Gourlan et al., 2010; Pena et al., 2005), although more evidence is required to test the significance of this observation. Overall, the HH-leach seems to be very effective in the dissolution of Mn oxyhydroxides and quite effective in the dissolution of Fe oxyhydroxides if carbonates are not present (anymore). The Ac-leach, in contrast, appears to be effective in the dissolution of some but not all Mn oxyhydroxides and relatively ineffective in the mobilisation of Fe oxyhydroxide phases.

In the Ac-leach series we observed a distinct peak in REE concentrations throughout all samples in the first leaching step in which the leachate was not saturated with Ca anymore, i.e. in which the Ca concentration is significantly lower than the maximum observed in the previous leaching steps (cf. Fig. 4 (a) and S.1). Remarkably, this peak in REE concentrations does not coincide with a comparable trend in Mn, Fe or Al concentrations. A similar behaviour is only apparent in HREE/LREE, which show a marked reduction during this peak in 12 out of 19 cases, and a marked increase in sample 2 CT. In the MREE/MREE* ratio a moderate reduction is observable in a few cases. The lowest Nd/Ca ratios in our early Ac-leaches are comparable to those observed by Palmer (1985) in the calcite lattices of chemically cleaned foraminifera tests ($6 \pm 4 \times 10^{-7}$, n = 20). Two different lines of reasoning could explain this behaviour of the REE in the Ac-leach series. The first is that the dissolution of the REE compounds is effectively prevented at the beginning of the leaches when there is an excess of carbonate present in the sediment, compared to the dissolution capacity of the leach. They would then only be effectively released once the carbonate does not buffer the acid in the leach sufficiently anymore, similar to the Fe oxyhydroxides in the HH-leaches. The second possibility is that the REE are dissolved together with the Mn at the beginning of the Ac-leach series, but are reprecipitated on the particle surfaces in the sediment and leach dispersion during the leaching process. Thus, the REE are only extracted effectively during the dissolution of the calcite itself onto which they were readsorbed during previous leaching steps. This mechanism could explain why a similar effect cannot be observed in the course of the HH-leaches, even in the few samples for which this stronger leach is saturated with Ca: The EDTA included in the HH-leach effectively prevents the readsorption of the REE onto the remaining sediment, as it is actually meant to do and which was originally suggested by Gutjahr et al. (2007) and Wilson et al. (2013), for example.

4.1.3. Quantification of Nd contributions from different sediment fractions

The Nd isotope signatures of the first HH-leaches of the ordinary samples, as well as those from most Ac-leaches match those from picked foraminifera very closely (see Fig. 7, average difference of 1st HH-leach to foraminifera ε_{Nd}: -0.22 ± 0.60, 1SD, n = 16). Strikingly, this is also observed at sites where volcanogenic sediment components present a known contaminant for conventional leaches (Elmore et al., 2011). Radiogenic contamination in these sediments is only evident during the later stages of the leaching sequence, in the conventional leaches from Elmore et al. (2011), in the AcHH-leaches (Fig. 6), and in the leaches of sample 7 ASH from the beginning. However, foraminiferal and initial leach Nd isotope signatures do often not match those of regional deep water, especially in the northern North Atlantic, which was also observed by Elmore et al. (2011). This may have a number of different reasons. Firstly, while a minor contamination from detrital material cannot be completely excluded, it seems unlikely that such a contamination yields the same shift of the extracted Nd isotope signature in cleaned and uncleaned foraminifera of Elmore et al. (2011) on the one hand and uncleaned foraminifera and both different leaches in our this study. Another possibility would be a temporal variation of the local deep water ε_{Nd} which is not covered by the deep water measurements, and may be more pronounced in the northern North Atlantic, where a range of water masses with different Nd isotope compositions mix. Furthermore, we do not have a sufficiently constrained age control for our core top samples to verify that they correspond to recently sedimented material. Although, as stated in 2.1, several palaeoceanographic reconstructions suggest that the Nd isotope signatures in the Atlantic Ocean did not change significantly during the late Holocene, variations may still have occurred. Finally, considering that deviations from the seawater Nd isotope ratios are largest at the sites around Iceland, which are all towards more radiogenic signatures, an influence of pore water which has taken up Nd from young volcanogenic material in the sediment cannot be excluded (Abbott et al., 2015a; Rousseau et al., 2015). Pore water could thus be a medium that promotes an exchange of Nd from detrital sources with the hydrogenetic fraction of the sediment without letting all the detrital Nd escape to the bottom water. Although it is impossible to make a clearer distinction of the controlling mechanisms based on our data, for the reconstruction of past deep water Nd isotope signatures it should be kept in mind that an exchange of detrital and archived hydrogenetic Nd via pore waters may occur, especially in areas where reactive volcanogenic material is common.

Sample 1 TII is the only case where a significant unradiogenic offset of the Nd isotope ratio in leaches compared to the foraminifera value is found ($\Delta\varepsilon_{Nd} \approx -2$), which is also the largest absolute offset. While this cannot be a contamination with volcanogenic material, it is difficult to assess what may have caused this large discrepancy in this one case. We will thus continue to use this sample in the assessments in Section 4.3, yet not discuss it in detail because based on our complete data set it rather represents an outlier which is heavily dependent on the measurement of the corresponding foraminifera sample. Similarly, the large radiogenic offset in sample 7 ASH is based on a foraminifera sample from a neighbouring sediment core. While we think that the actual local deep water Nd isotope signature during the deposition of the ash layer should be similar to that foraminifera sample, the absolute value of the discrepancy between the foraminifera and leach signature may

be overestimated, for example due to interaction between reactive volcanogenic material and pore waters.

The samples of sites 1 to 4 and sample 7 ASH clearly demonstrate the effect of volcanogenic contamination. In the core top sediments of sites 3 and 4 leached Nd isotope compositions reach ε_{Nd} values of up to +4 during progressive leaching. Roberts and Piotrowski (2015) reported values of +4.3 ± 0.1 for the Nd isotope signature of Last Glacial Maximum (LGM) age volcanogenic grains from North-East Atlantic sediments. Under glacial sedimentation such volcanogenic material is commonly delivered to the northern North Atlantic as IRD from Iceland (Bond et al., 2001). Given the lack of other highly radiogenic sources in the North Atlantic realm, it is reasonable to assume that this value represents a realistic estimate of the end member for volcanogenic material in the northern North Atlantic. In all cases where a significant trend of the extracted Nd isotope signature occurs during progressive leaching, this trend is towards more radiogenic values (Fig. 6). The signatures of the detrital components are, however, distributed above and below the hydrogenetic ones (Fig. 6, black squares). We thus conclude that the actual non-volcanogenic detrital material does not get leached significantly and leaching of volcanogenic components in the sediments dominates the contamination of the extracted Nd isotope signatures, as has been observed by Wilson et al. (2013) at sediments from the Indian Ocean and by Molina-Kescher et al. (2014b) in the Pacific Ocean. Similarly, Vance et al. (2009) and Dessert et al. (2003) compiled data suggesting that basalts are among the most easily weathered rocks, even more so, if they are young. This observation implies that a simple comparison between the bulk detrital and leached Nd isotope composition (as is commonly done) is not a reliable validation of the hydrogenetic nature of the latter, because the detrital material is often too heterogeneous to be characterised by a measurement of the bulk residue.

We can provide a gross budget of the contributions of three different leachable end members to the Nd isotope signature extracted by our progressive HH-leaching. Here we adopt the Nd isotope ratio of the foraminifera samples as the true hydrogenetic value for each sample. The bulk detrital source can be divided into a volcanogenic component end member with the abovementioned radiogenic isotope signature of $\varepsilon_{Nd} = +4.3$, and the remaining detritus is characterised by the signature of the completely dissolved residual material after the complete HH-leach series (TD). We assume a two component mixture without residual material contribution for the first part of the leaching sequence and parameterise the reduction of the absolute quantity of leached Nd from the hydrogenetic source as a stable exponential decrease for a subsequent three end member mixing. We choose an exponential parameterisation for two reasons: Firstly, the Nd concentration decreases more or less exponentially at the beginning, where the Nd isotope ratio remains close to the seawater value. And secondly, it seems natural in a first order approach that the amount of hydrogenetic Nd extracted is proportional to the amount of hydrogenetic Nd remaining in the sediment. We start the exponential parameterisation of the hydrogenetic contribution at the earliest leaching step where the resulting total leached Nd is consistent with the measured value, i.e. where the necessary Nd from the three end members does not exceed the actually extracted Nd. This point is reached after the second to fourth leach and indicated as black arrows in Fig. 8. The set of equations we use describe a simple mixing relation:

$$c_{tot} = c_{hydr} + c_{volc} + c_{det} \tag{8}$$

$$c_{tot}\,\varepsilon_{tot} = c_{hydr}\,\varepsilon_{hydr} + c_{volc}\,\varepsilon_{volc} + c_{det}\varepsilon_{det} \tag{9}$$

Here, c denotes the Nd concentration derived from the respective fractions, which are the total, hydrogenetic, volcanogenic, and detrital phases. For the initial two end member case c_{det} is assumed to be zero.

We apply these end member calculations to the HH-leaches of the five core top sediments from the northern North Atlantic, sample 3 TII, and the ash turbidite sample. These samples exhibit a significant radiogenic alteration and all necessary data are available. The simple calculations (Fig. 8) show that the amount of Nd extracted from the volcanogenic component in the complete HH-leach series of samples 1 to 4 CT lies in a narrow range between 1.1 and 1.8 μg per g bulk sediment, or 18 to 26% of the total leached Nd. In terms of dissolved material, we estimate this to about 5 to 9% of leached volcanogenic material (relative to the total sample mass assuming a Nd concentration of 20 ppm in volcanogenic particles, similar to Roberts and Piotrowski, 2015). The actual Nd content of volcanogenic material, however, may vary significantly. For example, Kempton et al. (2000) found concentrations between 2 and 40 ppm Nd in basalts from the North Atlantic Igneous Province and our numbers are thus only a gross estimate. The remaining detrital contribution to the leached Nd makes up about 10%

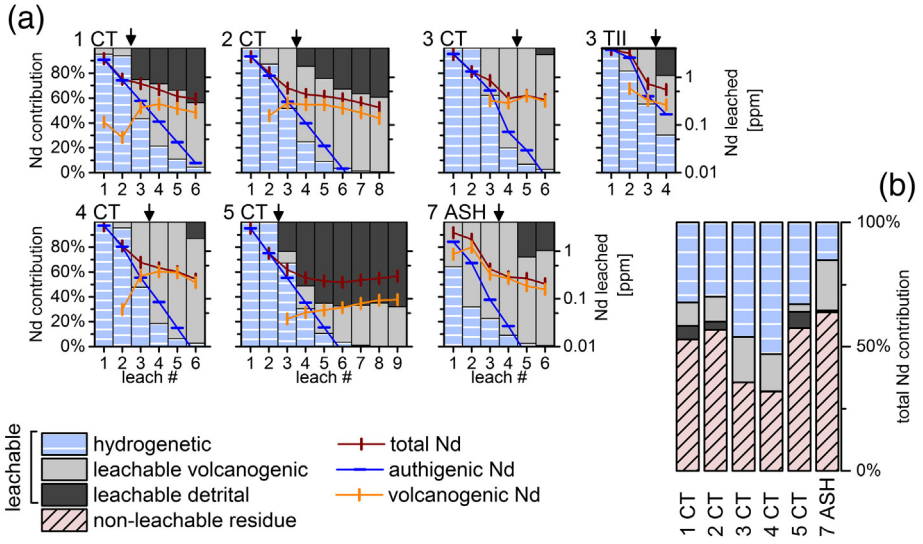

Fig. 8. Calculated three end member contributions to the extracted Nd isotope signatures of the HH-leaches. (a) Calculated relative Nd contributions of the three endmembers (columns normalised to the total Nd extracted per leach in %, left axis) and absolute Nd contributions (lines, right y-axis, in ppm) as calculated and parameterised by the end member calculations described in the text. The amount of volcanogenic Nd in the leachate is negligible where the orange line is not shown. The black arrows indicate the point at which the calculations are switched from two- to three end members with the hydrogenetic contribution being set as an exponentially decreasing contribution. (b) Overall distribution of Nd in the six modelled samples accounted for by the three identified leachable end members and the non-leachable detritus. The isotope ratios and elemental abundances of the 7th leach of samples 2 and 5 CT are interpolated from leaches 6 and 8.

and 7% at sites 1 and 2, but is negligible at sites 3 and 4. In sample 5 CT the volcanogenic Nd amounts to 8% and the contribution from detrital Nd is relatively high with 18%. In sample 7 ASH, the volcanogenic Nd contribution in the first leach, which is evidently offset, is already 36%. This is the only sample where the amount of extracted volcanogenic Nd in the course of the whole procedure outweighs the hydrogenetic component by one third. This corresponds to 15% of this sample's mass being leachable volcanogenic material (where 'leachable' means that it is extracted with 10 HH-leaches). Alternatively, if the hydrogenetic component has been altered by partial dissolution of volcanogenic material in the pore waters, about one third of the modified hydrogenetic Nd originates from the volcanogenic source. Note that in these calculations the contribution from the detrital component is most uncertain, since, as already mentioned, the detritus is probably not as homogeneous as assumed, neither in reactivity nor in Nd isotope composition and Nd concentration. We further calculate that due to the partial leaching of the detrital volcanogenic phases, the original bulk detrital Nd isotope signature was offset by 1 to 2.5 ε_{Nd} units towards less radiogenic values. This may be important for sediment provenance studies, in which the authigenic fraction is commonly removed with acidic solutions. It is worth mentioning that other possible parameterisations for the course of the extraction of hydrogenetic Nd mainly affect the amount of detrital Nd leached. A scenario with significantly different contributions of these three end members would require considerable contribution from the detrital fraction already at the start of the leaching sequence. Due to the high reactivity of the carbonate fraction and the abovementioned lack of correlation between detrital Nd isotope signatures and the Nd isotope trend under progressive leaching we consider such a case unlikely.

Fig. 9 demonstrates the correlation of the contribution of volcanogenic Nd to the extracted Nd signal with the (remaining) calcium carbonate content of the sample (Fig. 9 a) and with the ratio of remaining calcium carbonate to remaining leachable volcanogenic material in the sample (Fig. 9 b). Both relationships have to be interpreted with care because other factors such as the amount of hydrogenetic Nd that was already leached or the sediment composition certainly also exert some effects. However, the positive relationship in plot (b), especially once there is more volcanogenic material in the sample than calcium carbonate (left of 1 on the x-axis), is another indication that the reaction of the leaching solution with volcanogenic components in the sediment is effectively impeded by the preferential dissolution of carbonates in the sediment. This result is supported, for example, by the observations from Gislason and Oelkers (2003), who found differences in the dissolution rate of basaltic glass of more than an order of magnitude higher at pH = 4 compared to pH = 6, which is the pH range prevailing in our leachates (depending on the $CaCO_3$ content of the sample, see S.4). Our end member calculations are further supported by a comparison of the results with the europium anomaly in the leachates and the total digestions. Fig. 9 (d) shows that the negative Eu/Eu* in these samples clearly originates from a leachable volcanogenic source. Combined with a tentative depletion in the HREE (cf. S.2 and S.3), this points to the dissolution of basaltic volcanogenic glass during the progressive leaching (Sinha, 1982). The TD data of these samples, on the other hand, exhibit positive Eu anomalies, often together with elevated Nd isotope signatures, indicating that plagioclase remained in the residue (Weill and Drake, 1973). For sample 7 ASH a content of at least 5% plagioclase in the sediment is reported (Jantschik, 1991). Therefore, we conclude that basaltic glass is partially dissolved with the acid-reductive leaches, especially at low pH, whereas glauconite mostly remains in the residue. However, due to the buffering effect of carbonate and the high concentration of easily leachable hydrogenetic Nd, the contamination from volcanogenic glass can be evaded and overprinted. Leaching at a higher pH, with less leach solution or with a shorter reaction time may therefore be an effective way to counteract volcanogenic contamination, but may have to be tested for its effectiveness by comparison with seawater signatures and

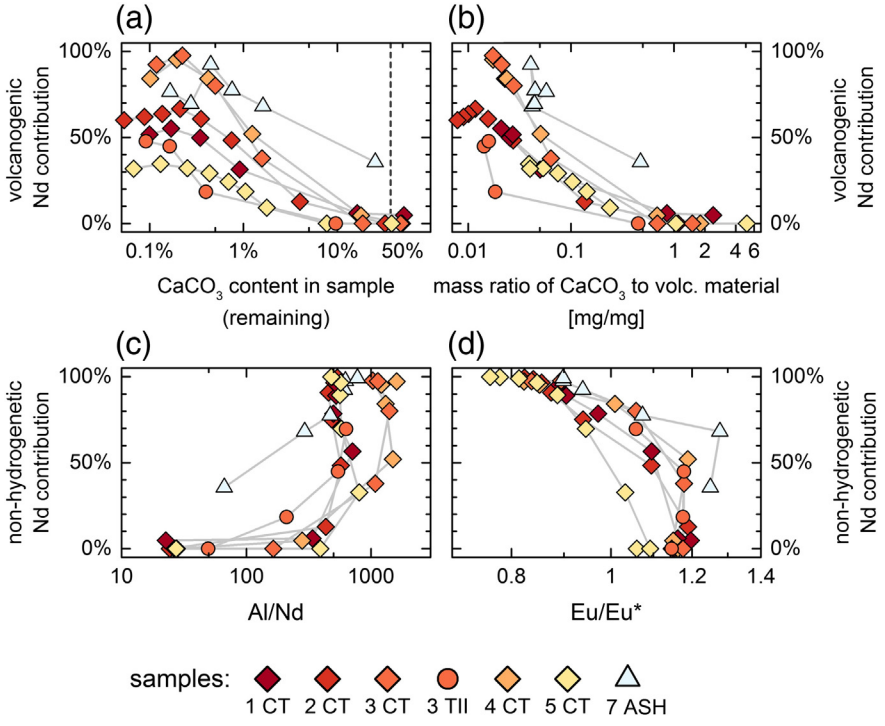

Fig. 9. Calculated three end member contributions to the extracted Nd isotope signatures of the HH-leaches in relation to the sediment composition and calculated Nd sources. (a) Calculated relative contribution of volcanogenic sources to the Nd signal vs. calcium carbonate content in the sample at the start of the respective leach. The vertical dashed line marks the amount of $CaCO_3$ that can be extracted with one HH-leach. (b) Calculated relative contribution of volcanogenic sources to the Nd signal vs. ratio of calcium carbonate to leachable volcanogenic material mass contained in the sediment at the start of the respective leach. (c) & (d) Correlation of the relative contribution of Nd from all leachable detrital sources with the Al/Nd ratio and the europium anomaly in the leachate. Note that all x-axes are logarithmic. Colour codes are the same as in Fig. 10. The isotope ratios and elemental abundances of the 7th leach of samples 2 and 5 CT are interpolated from leaches 6 and 8.

foraminiferal Fe-Mn oxyhydroxide phases on a site by site basis due to differences in bulk sediment composition. This effect also explains why conventional leaching methods, where the sediment is completely decarbonated in a first step, suffer from volcanogenic contamination. It also agrees with the conclusions of Wilson et al. (2013) who observed variable degrees of volcanogenic contamination depending on the ratio of solution volume to sample mass and on the degree of decarbonation prior to their HH-leach (see also Molina-Kescher et al. (2014b) for the latter). In our samples, significant volcanogenic contamination was prevented as long as there was at least half as much carbonate present in the sample as was leachable volcanogenic material (data in Fig. 9 (b) with $x > 1/2$).

4.2. The influence of non-biogenic carbonates

As shown above, calcium carbonate is the first fraction to be dissolved during acid-reductive leaching. While this seems not to be an issue for the extracted Nd isotope signal in the case of biogenic carbonates as discussed, it can present a problem if detrital or authigenic carbonates are present in the sediment. Such carbonates may contain higher amounts of Nd, extreme Nd isotope signatures or react differently, thus presenting a potentially significant source for non-hydrogenetic contamination in leaching methods where carbonates are not completely removed beforehand. Both authigenic and detrital carbonate have been linked to low Sr/Ca ratios compared to biogenic carbonates, which will become relevant later (Channell et al., 2012; Jantschik, 1991).

The sediment composition of sample 7 IRD is dominated by IRD deposition together with the (presumably post-depositional) recrystallisation of carbonate and precipitation of authigenic dolomite in the pore water, as described by Jantschik (1991). Results from this sample are also distinct from the others given that extremely unradiogenic Nd isotope signatures as low as $\varepsilon_{Nd} \approx -25.5$ were extracted in both first leaches. The least radiogenic waters in the modern Atlantic deeper than 3000 m, however, show $\varepsilon_{Nd} \approx -15$ (Lacan et al., 2012), and Roberts and Piotrowski (2015) reconstructed values as high as −8 during Heinrich Stadial 1 from a sediment core 7° north of our site 7. Furthermore, the Nd isotope signature of the residual total digestion in sample 7 IRD ($\varepsilon_{Nd} = -26.4$, Fig. 6) is very close to that of the initial leaches. Although the first Ac- and HH-leaches are almost identical, the subsequent three HH-leaches are offset by about $+4\ \varepsilon_{Nd}$ units, whereas the same Ac-leaches show a gradual change by $+1\ \varepsilon_{Nd}$ unit per step. It is very unlikely that these unradiogenic signatures reflect a true local oceanic deep water mass signal. They rather correspond to the Nd signatures of the IRD, which was delivered from the Laurentide Ice Sheet (Hemming, 2004; Jantschik, 1991). Due to the concomitant dissolution of authigenic carbonates during leaching as indicated by the low Sr/Ca ratios (cf. S.2), we conclude that it is either the Nd from dolomites or other authigenic phases precipitated from the pore water dominating the Nd isotope signature of the leachate. The pore water ε_{Nd} must therefore have re-equilibrated with the Nd isotope signature from the IRD, which can occur via dissolution of less resistant phases like detrital carbonates, commonly delivered from the Laurentide Ice Sheet during IRD events (Bond et al., 1992), or partial leaching of the bulk IRD. The shift towards more radiogenic ε_{Nd} during progressive leaching could then be a contribution from an actual deep water derived Nd isotope signal. This seawater signal, however, may itself have been altered by the massive flux of IRD to the seafloor during Heinrich Stadial 1, as was recently similarly suggested by Roberts and Piotrowski (2015). As a bottom line, the leached Nd isotope signal in this IRD-rich layer is altered by an easily leachable unradiogenic sediment fraction, which is an example for contamination by a non-volcanogenic phase.

Authigenic carbonates as in sample 7 IRD do not commonly form in deep sea sediments and are usually a sign for extreme sedimentary environments. Their composition and thus chemical behaviour may furthermore strongly depend on the local conditions under which they precipitated. In principle, authigenic carbonates should only contain Nd from the pore waters, which in turn should have been leached from the sediment itself and mixed with ambient bottom water. As long as the detrital fraction was chemically resistant enough not to be significantly affected by in situ leaching, the authigenic carbonate signal should only lead to a smearing of the originally archived deep water Nd isotope signal. If, however, the detritus were leached (partially) and released Nd into the pore waters from which the authigenic carbonates precipitated, then these present a potential source of contamination (Abbott et al., 2015b). It is worth noting that in sediments in which authigenic carbonates formed, foraminifera may have been dissolved, so that neither leaching the sediment nor picking of foraminifera are viable options for the extraction of a reliable deep water Nd isotope signature, as is evident from sample 7 IRD. Roberts and Piotrowski (2015) picked and analysed detrital carbonate grains from a Heinrich 1 IRD layer and found a Nd content of 0.8 ppm with $\varepsilon_{Nd} = -18.6 \pm 0.2$. The first HH-leaches of our study contain at least 2 μg Nd per g bulk sediment. Assuming that a shift of the extracted Nd isotope signature of $>0.5\ \varepsilon_{Nd}$ units should be avoided and the true seawater signature is $\varepsilon_{Nd} = -10$ requires the sediment to contain <15% detrital carbonate with the above Nd content. This is a worst case scenario in which all detrital carbonate is dissolved during that first leach. Fortunately, such high concentrations of detrital carbonate are unlikely to be found far from continental margins or IRD belts.

4.3. Elemental ratios as proxies for non-hydrogenetic contamination

In earlier studies it was proposed to use either the Al/Nd ratio in leachates (Gutjahr et al., 2007) or REE patterns (Bayon et al., 2002; Martin et al., 2010) as proxies for the origin of the Nd in the leachate, i.e. as proxies for potential contamination of the extracted signal by non-hydrogenetic sources. Since we observe significant and variable degrees of radiogenic contamination in several samples, these element ratios should correlate with the offset of the Nd signature from the foraminiferal value, if they are appropriate tracers of contamination in our samples. We simulate leaches of variable strength by integrating our Nd isotope and concentration data from the first to the nth leach for each sample, where $n = 1$ represents the weakest and $n = 10$ the strongest leach. Cross-plots of Al/Nd, the REE parameters, and additionally Sr/Ca versus the Nd isotope offset of these integrated signals during progressive leaching are plotted in Fig. 10. We included Sr/Ca because for a method where carbonates are not removed from the sediment before leaching, this ratio could in principle be a valuable indicator for the dissolution of detrital or authigenic carbonates, which can be depleted in Sr as already mentioned. In this study, however, we did not find any evidence for detrital carbonate dissolution, except in sample 7 IRD, as discussed above.

The Al/Nd ratio in the HH-leachates shows large variability with integrated values ranging from 14 to 480 (values up to 4.2×10^3 were measured in individual HH-leaches and between 3.3×10^3 and 1.1×10^3 in the residues). Correlation coefficients of the integrated Nd isotope signature with integrated Al/Nd ratios are high ($r = 0.94 \pm 0.1$; 1 S.D.; $n = 17$) for individual samples (including the two extraordinary samples), except the two from site 10. The few measured Nd isotope ratios of samples 10 CT and 10 TII do not vary significantly, and thus the correlation is weak. Taking all data points of the ordinary samples together, the correlation is somewhat weaker ($r = 0.73$, $n = 79$), but still highly significant. The weaker correlation can possibly be explained by the fact that the change of the Nd isotope composition from a given degree of contamination depends on the difference of the isotope composition in the end members. The more unradiogenic the hydrogenetic isotope composition is, the larger the change in ε_{Nd} caused by contamination will be. Yet, the correlation across samples from different geographical areas and sedimentological composition leached with varying intensity (i.e. across the stages of our progressive leaching) indicates the possibility to predict contamination in the

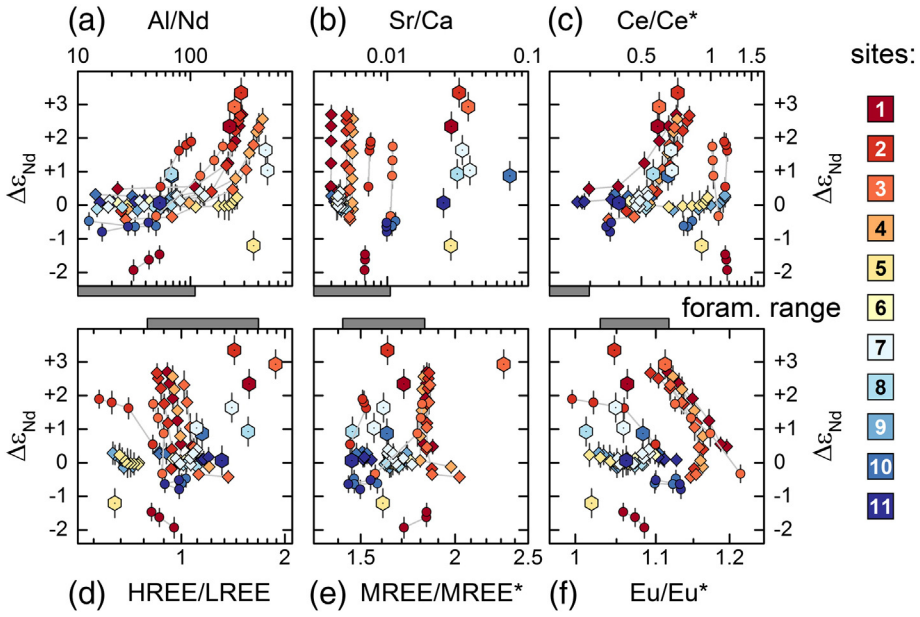

Fig. 10. Cross-plots of the Nd isotope signature offset versus geochemical proxies for contamination. Both isotope and elemental ratios are integrated from the 1st to the nth HH-leach in order to investigate the changes with variable degree of leaching. The offset is defined as the difference of leached aliquots in relation to foraminiferal signatures. Included are HH-leaches (CT: diamonds, TII: circles) and AcHH-leaches (hexagons, all CT). Lines between data points are included to indicate the consecutive leaches from the same sample. The colour codes the different sites from North (dark red) to South (dark blue). Grey bars below and above the x-axes in the centre of the figure mark the range of the respective ratio measured in the picked foraminifera across all samples from this study. (a) Al/Nd as a proxy for detrital contamination as proposed by Gutjahr et al. (2007). (b) Sr/Ca as a proxy for the dissolution of detrital carbonates. (c) to (f) REE parameters as proxies for the origin of REE (e.g. Martin et al., 2010). All x-axes are logarithmic in scale. (For interpretation of the references to colour in this figure legend, the reader is referred to the web version of this article.)

extracted Nd isotope composition from the Al/Nd ratio. According to the data of our ordinary samples, we can estimate that an Al/Nd ratio lower than roughly 100 minimises the probability of detrital contamination in the leachate (with the exceptions of samples 1 and 2 TII). A higher ratio, however, does not necessarily mean a significant contamination, as can be seen from sample 5 CT, for example. Similarly, our foraminifera samples exhibit Al/Nd values below 110 and thus within the range for which no significant Nd isotope offsets in the leaches were observed. It is important to note, however, that this correlation is much weaker in the case of the AcHH-leaches and therefore presumably also for conventional leaches with prior carbonate removal. Furthermore, not adding EDTA as a chelating agent will change the extracted Al/Nd for reductively leached samples due to partial re-adsorption of hydrogenetic Nd (cf. Gutjahr et al., 2007 Table 5 vs. Gutjahr et al., 2010 Table 2 and Wilson et al., 2013). Moreover, it has to be kept in mind that ferromanganese oxyhydroxides do also contain some hydrogenetic Al (Gutjahr et al., 2014; Koschinsky and Halbach, 1995) and thus the mere presence of trace Al in the leachate does not necessarily indicate detrital contamination. Indeed, Fig. 9 (c) could point to the mobilisation of hydrogenetic Al, since the Al/Nd ratio in the leachates rises at the beginning, without a concomitant rise in the contribution of detrital Nd.

Compared to the Al/Nd ratio the REE parameters in Fig. 10 (c)–(f) do not appear as useful as indicators of contamination. While there is a considerable correlation of the shift in Nd isotope compositions and the cerium anomaly in individual samples, no significant overarching correlation can be found across the samples. Similarly, as discussed above, a correlation of Nd contamination with HREE and europium depletion can be found in the samples from the northern North Atlantic due to the dissolution of basaltic glass. Such a correlation, however, is not present in all the samples and neither are the values in HREE/LREE or Eu/Eu* in the contaminated samples unique. Thus, these ratios cannot be used to identify detrital contamination without further information. A strong discrepancy in HREE/LREE between the HH-leaches and AcHH-leaches from the same sediment is found. This indicates that other factors than the degree of detrital dissolution exert an effect on the slope of the REE pattern in the leachate, which does not manifest in the other REE parameters. The readsorption of REE to the sediment during the preceding Ac-leaches, for example, could lead to the observed increase in HREE in the AcHH-leaches. Alternatively, the cause could be the pH (i.e. the carbonate content) or the elemental composition of the (remaining) Fe-Mn oxyhydroxides themselves, which may change during the leaching sequence due to preferential dissolution of Mn-oxides over Fe-oxides, as discussed above. We find no significant correlation of $\Delta\varepsilon_{Nd}$ and MREE/MREE*. Thus, without further information, the REE patterns cannot be constrained well enough with our data in order to use them as an operational indicator for contamination.

In this discussion we focused on the identification of non-hydrogenetic contamination based on a variety of individual samples without further information. However, we want to point out that the correlations between these elemental ratios and the offsets in Nd isotope compositions are much more significant when we look at samples from geographical proximity (i.e. sedimentology) and age. We thus suppose that the informational value of these parameters is significantly increased if actual depth records are produced from sediment cores. By comparing the variation of the elemental ratios and the Nd isotope signatures over sediment depth, assessments of contaminations and their possible causes in individual sediment layers are supposedly more accurate than with individual samples taken out of context. In such more localised investigations, the REE patterns and Sr/Ca ratio may prove to add valuable information about the origin of the extracted Nd. Based on the variations in our individual samples (Fig. 10), contamination should then be accompanied by increases in Al/Nd and Ce/Ce* or decreases in Sr/Ca, HREE/LREE, and Eu/Eu*.

4.4. Implications for an improved and reliable acid-reductive leaching method

Based on the results of this study we propose a modified and simplified leaching procedure for the reliable extraction of hydrogenetic Nd from carbonate bearing pelagic sediments (see supplementary material S.5). Similar to what has been proposed before (e.g. Haley et al., 2008; Gourlan et al., 2010; Wilson et al., 2013), we show that our first weak

HH-leaches without prior carbonate removal reliably extracted a foraminifera-like Nd isotope signature from pelagic deep sea sediments. We show that this holds in samples containing at least half as much $CaCO_3$ as leachable volcanogenic material (Fig. 9 a and b) and as long as there is no substantial contribution from detrital or authigenic carbonates. The fact that our results agree with those from Wilson et al. (2013), who carried out quite different experiments, and that other authors managed to reliably extract hydrogenetic Hf isotope compositions from clayey sediments in the Arctic (Chen et al., 2012; Haley et al., 2008) substantiates that gentle reductive leaching as suggested here should be capable of extracting a reliable bottom water Nd isotope signal at many deep sea locations away from major continental input sources. This method was not tested with sediments containing only negligible amounts of carbonate, but our data suggest that weak HH-leaches could release radiogenic Nd from reactive volcanogenic material if present in carbonate free sediment. As a quality check for the sediment leaches we propose the additional measurement of the Al/Nd ratio in the leachate, which sensitively indicates contributions of volcanogenic or other detrital contaminant phases. Furthermore, the Sr/Ca ratio may be a useful indicator for contamination from detrital or authigenic carbonate, but this could not be tested comprehensively with the available samples. Increasing the pH, using less acid, less solution, and/or adding synthetic carbonate as a buffer may further reduce the susceptibility to contamination by both non-biogenic carbonates and volcanogenic detritus, but requires further testing. It is therefore recommended to compare the Nd isotope signatures of sediment leaches with the foraminiferal signal, in particular in complex sedimentary settings.

5. Conclusions

We investigated the processes during progressive leaching with either buffered acetic acid or with acetic acid in combination with a chelating and a reducing reagent. Our results have important implications for the applicability of the techniques to extract the hydrogenetic Nd isotope signature from bulk marine sediments.

The succession of different phases being mobilised within our leach sequences shows that Nd isotope signatures at the beginning of the leaching process agree well with those from foraminifera samples. Previous work suggests that sedimentary foraminifera record and preserve a true seawater Nd isotope ratio (Elmore et al., 2011; Roberts and Piotrowski, 2015; Roberts et al., 2012) and our new data show that the same holds for our weak HH-leaches. Importantly, this is also the case for samples which suffered from volcanogenic contamination released during conventional leaching (i.e. including prior removal of carbonate). Significant contamination by non-hydrogenetic phases occurs only after the buffering effect of the sedimentary carbonates is reduced significantly. Our results support previous suggestions that contaminant Nd is released preferentially from volcanogenic detritus during the leaching procedure and our REE data suggest that this phase is basaltic glass. Other lithogenic phases do not seem to be relevant contaminant sources of the extracted Nd isotope signatures.

The analysis of different parameters for the validation of a purely hydrogenetic origin of the extracted Nd isotope signature shows that increased Al/Nd ratios in the leachate covary with detrital contaminations, as suggested by Gutjahr et al. (2007). REE ratios behave less consistent and are therefore inappropriate for the identification of contamination in an individual sample. However, they may prove to be valuable for the assessment of the origin of the leached REE in studies focusing on better confined sedimentological settings. Whether contamination of the leachate by detrital or authigenic carbonates may or may not be detectable with the measurement of Sr/Ca ratios remains to be tested. In general, an increase of the pH in the leachate or a decreased reaction time of the leaching reagent with the samples may further reduce the risk of contamination both by volcanogenic material and non-biogenic carbonates. Such a modification should thus allow the application to sediments completely devoid of carbonates but with a volcanogenic component, which was, however, not tested here.

We propose a refined leaching method that is simple to use, applicable to a wide range of deep sea sediments, and less time consuming than other procedures to retrieve deep water Nd isotope signatures. This opens the door to a higher temporal and spatial coverage and resolution of this proxy and will improve our understanding of deep ocean circulation and continental chemical weathering.

Acknowledgements

Sediment material for this study was provided by the ODP/IODP core repository Bremen and the core repository of the University of Tübingen. Walter Hale, Hartmut Schulz, Margret Bayer, and Hartmut Heinrich are thanked for their expertise in sample selection and handling. We thank Silvia Rheinberger and Christian Scholz for help with the ICP-OES measurements and Stefan Rheinberger, René Eichstädter, and Benny Antz for help in the lab and assistance in ICP-QMS measurements. Finally, we thank Mike William, Sanam Vardag, and the Physics of Environmental Archives working group in Heidelberg for fruitful discussions. This project was supported financially through grant FR1341/3 by the Deutsche Forschungsgemeinschaft. Jörg Lippold was supported by the FP7-PEOPLE-2013-IEF, Marie Curie proposal 622483 and grant LI1815/4 by the Deutsche Forschungsgemeinschaft. Editorial handling by Prof. Michael E. Böttcher is acknowledged. We are grateful for the constructive reviews by two anonymous reviewers and particularly David Wilson that helped improving an earlier version of the manuscript.

Map. KMZ file containing the Google Map of the most important areas described in this article.

Appendix A. Supplementary data

Supplementary data associated with this article can be found in the online version, at doi: http://dx.doi.org/10.1016/j.chemgeo.2016.06.024. These data include the Google Map of the most important areas described in this article.

References

Abbott, A.N., Haley, B.a., McManus, J., Reimers, C.E., 2015a. The sedimentary flux of dissolved rare earth elements to the ocean. Geochim. Cosmochim. Acta 154, 186–200. http://dx.doi.org/10.1016/j.gca.2015.01.010.

Abbott, A.N., Haley, B.A., McManus, J., 2015b. Bottoms up: Sedimentary control of the deep North Pacific Ocean's ε_{Nd} signature. Geology 43, G37114.1. http://dx.doi.org/10.1130/G37114.1.

Abouchami, W., Galer, S.J.G., Koschinsky, A., 1999. Pb and Nd isotopes in NE Atlantic Fe-Mn crusts: proxies for trace metal paleosources and paleocean circulation. Geochim. Cosmochim. Acta 63, 1489–1505. http://dx.doi.org/10.1016/S0016-7037(99)00068-X.

Alvarez Zarikian, C.A., Stepanova, A.Y., Grützner, J., 2009. Glacial-interglacial variability in deep sea ostracod assemblage composition at IODP Site U1314 in the subpolar North Atlantic. Mar. Geol. 258, 69–87. http://dx.doi.org/10.1016/j.margeo.2008.11.009.

Bau, M., Koschinsky, A., Dulski, P., Hein, J.R., 1996. Comparison of the partitioning behaviours of yttrium, rare earth elements, and titanium between hydrogenetic marine ferromanganese crusts and seawater. Geochim. Cosmochim. Acta 60, 1709–1725. http://dx.doi.org/10.1016/0016-7037(96)00063-4.

Bayon, G., German, C.R., Boella, R.M., Milton, J.A., Taylor, R.N., Nesbitt, R.W., 2002. An improved method for extracting marine sediment fractions and its application to Sr and Nd isotopic analysis. Chem. Geol. 187, 179–199. http://dx.doi.org/10.1016/S0009-2541(01)00416-8.

Bayon, G., German, C.R., Burton, K.W., Nesbitt, R.W., Rogers, N., 2004. Sedimentary Fe-Mn oxyhydroxides as paleoceanographic archives and the role of aeolian flux in regulating oceanic dissolved REE. Earth Planet. Sci. Lett. 224, 477–492. http://dx.doi.org/10.1016/j.epsl.2004.05.033.

Böhm, E., Lippold, J., Gutjahr, M., Frank, M., Blaser, P., Antz, B., Fohlmeister, J., Frank, N., Andersen, M.B., Deininger, M., 2015. Strong and deep Atlantic meridional overturning circulation during the last glacial cycle. Nature 517, 73–76. http://dx.doi.org/10.1038/nature14059.

Bond, G., Heinrich, H., Broecker, W., Labeyrie, L., McManus, J., Andrews, J., Huon, S., Jantschick, R., Clasen, S., Simet, C., Tedesco, K., Klas, M., Bonani, G., Ivy, S., 1992. Evidence for massive iceberg discharges in the North Atlantic Ocean during the last glacial period. Nature 360, 249–345.

Bond, G., Kromer, B., Beer, J., Muscheler, R., Evans, M.N., Showers, W., Hoffmann, S., Lotti-Bond, R., Hajdas, I., Bonani, G., 2001. Persistent solar influence on North Atlantic climate during the Holocene. Science 294, 2130–2136. http://dx.doi.org/10.1126/science.1065680.

Bowles, J., 2006. Magnetostratigraphy and magnetic mineralogy of sediments from Walvis Ridge, Leg 208. Proc. Ocean Drill. Program Sci. Results 208. http://dx.doi.org/10.2973/odp.proc.sr.208.206.2006.

Boyle, E.A., 1983. Manganese carbonate overgrowths on foraminifera tests. Geochim. Cosmochim. Acta 47, 1815–1819. http://dx.doi.org/10.1016/0016-7037(83)90029-7.

Carter, P., Vance, D., Hillenbrand, C.D., Smith, J.A., Shoosmith, D.R., 2012. The neodymium isotopic composition of waters masses in the eastern Pacific sector of the Southern Ocean. Geochim. Cosmochim. Acta 79, 41–59. http://dx.doi.org/10.1016/j.gca.2011.11.034.

Channell, J.E.T., Hodell, D.A., Romero, O., Hillaire-Marcel, C., de Vernal, A., Stoner, J.S., Mazaud, A., Röhl, U., 2012. A 750-kyr detrital-layer stratigraphy for the North Atlantic (IODP sites U1302–U1303, Orphan Knoll, Labrador Sea). Earth Planet. Sci. Lett. 317-318, 218–230. http://dx.doi.org/10.1016/j.epsl.2011.11.029.

Chen, T.-Y., Frank, M., Haley, B.A., Gutjahr, M., Spielhagen, R.F., 2012. Variations of North Atlantic inflow to the central Arctic Ocean over the last 14 million years inferred from hafnium and neodymium isotopes. Earth Planet. Sci. Lett. 353–354, 82–92. http://dx.doi.org/10.1016/j.epsl.2012.08.012.

Chester, R., Hughes, M., 1967. A chemical technique for the separation of ferro-manganese minerals, carbonate minerals and adsorbed trace elements from pelagic sediments. Chem. Geol. 2, 249–262. http://dx.doi.org/10.1016/0009-2541(67)90025-3.

Cohen, A.S., O'Nions, R.K., Siegenthaler, R., Griffin, W.L., 1988. Chronology of the pressure-temperature history recorded by a granulite terrain. Contrib. Mineral. Petrol. 98, 303–311. http://dx.doi.org/10.1007/BF00375181.

Colin, C., Frank, N., Copard, K., Douville, E., 2010. Neodymium isotopic composition of deep-sea corals from the NE Atlantic: implications for past hydrological changes during the Holocene. Quat. Sci. Rev. 29, 2509–2517. http://dx.doi.org/10.1016/j.quascirev.2010.05.012.

Copard, K., Colin, C., Douville, E., Freiwald, A., Gudmundsson, G., De Mol, B., Frank, N., 2010. Nd isotopes in deep-sea corals in the North-eastern Atlantic. Quat. Sci. Rev. 29, 2499–2508. http://dx.doi.org/10.1016/j.quascirev.2010.05.025.

Crocket, K.C., Vance, D., Gutjahr, M., Foster, G.L., Richards, D.A., 2011. Persistent Nordic deep-water overflow to the glacial North Atlantic. Geology 39, 515–518. http://dx.doi.org/10.1130/G31677.1.

Crocket, K.C., Vance, D., Foster, G.L., Richards, D.A., Tranter, M., 2012. Continental weathering fluxes during the last glacial/interglacial cycle: Insights from the marine sedimentary Pb isotope record at Orphan Knoll, NW Atlantic. Quat. Sci. Rev. 38, 89–99. http://dx.doi.org/10.1016/j.quascirev.2012.02.004.

Croudace, I., 1981. A possible error source in silicate wet-chemistry caused by insoluble fluorides. Chem. Geol. 31, 153–155.

Dessert, C., Dupré, B., Gaillardet, J., Francois, L.M., Allègre, C.J., 2003. Basalt weathering laws and the impact of basalt weathering on the global carbon cycle. Chem. Geol. 202, 257–273. http://dx.doi.org/10.1016/j.chemgeo.2002.10.001.

Elderfield, H., Greaves, M.J., 1982. The rare earth elements in seawater. Nature 296, 214–219. http://dx.doi.org/10.1038/296214a0.

Elmore, A.C., Piotrowski, A.M., Wright, J.D., Scrivner, A.E., 2011. Testing the extraction of past seawater Nd isotopic composition from North Atlantic deep sea sediments and foraminifera. Geochem. Geophys. Geosyst. 12. http://dx.doi.org/10.1029/2011GC003741.

Frank, M., 2002. Radiogenic isotopes: tracers of past ocean circulation and erosional input. Rev. Geophys. 40, 1001. http://dx.doi.org/10.1029/2000RG000094.

Frank, M., O'Nions, R.K., Hein, J.R., Banakar, V.K., 1999. 60 Myr records of major elements and Pb-Nd isotopes from hydrogenous ferromanganese crusts: reconstruction of seawater paleochemistry. Geochim. Cosmochim. Acta 63, 1689–1708. http://dx.doi.org/10.1016/S0016-7037(99)00079-4.

Frank, N., Waldner, A., Christophe, C., Montagna, P., Dubois-Dauphin, Q., Wu, Q., 2014. The Nd-isotopic fingerprinting of North Atlantic water masses and its influences from local sources such as Iceland.

Freslon, N., Bayon, G., Toucanne, S., Bermell, S., Bollinger, C., Chéron, S., Etoubleau, J., Germain, Y., Khripounoff, A., Ponzevera, E., Rouget, M.L., 2014. Rare earth elements and neodymium isotopes in sedimentary organic matter. Geochim. Cosmochim. Acta 140, 177–198. http://dx.doi.org/10.1016/j.gca.2014.05.016.

Gislason, S.R., Oelkers, E.H., 2003. Mechanism, rates, and consequences of basaltic glass dissolution: II. An experimental study of the dissolution rates of basaltic glass as a function of pH and temperature. Geochim. Cosmochim. Acta 67, 3817–3832. http://dx.doi.org/10.1016/S0016-7037(00)00176-5.

Goldstein, S.L., Hemming, S.R., 2003. Long-lived isotopic tracers in oceanography, paleoceanography, and ice-sheet dynamics. Treatise on Geochemistry. Elsevier, pp. 453–489 http://dx.doi.org/10.1016/B0-08-043751-6/06179-X.

Gourlan, A.T., Meynadier, L., Allégre, C.J., Tapponnier, P., Birck, J.L., Joron, J.L., 2010. Northern Hemisphere climate control of the Bengali rivers discharge during the past 4 Ma. Quat. Sci. Rev. 29, 2484–2498. http://dx.doi.org/10.1016/j.quascirev.2010.05.003.

Gutjahr, M., Frank, M., Stirling, C.H., Klemm, V., van de Flierdt, T., Halliday, A.N., 2007. Reliable extraction of a deepwater trace metal isotope signal from Fe-Mn oxyhydroxide coatings of marine sediments. Chem. Geol. 242, 351–370. http://dx.doi.org/10.1016/j.chemgeo.2007.03.021.

Gutjahr, M., Frank, M., Stirling, C.H., Keigwin, L.D., Halliday, A.N., 2008. Tracing the Nd isotope evolution of North Atlantic Deep and Intermediate waters in the western North Atlantic since the LGM from Blake Ridge sediments. Earth Planet. Sci. Lett. 266, 61–77. http://dx.doi.org/10.1016/j.epsl.2007.10.037.

Gutjahr, M., Hoogakker, B.A.A., Frank, M., McCave, I.N., 2010. Changes in North Atlantic Deep Water strength and bottom water masses during Marine Isotope Stage 3 (45–35 ka BP). Quat. Sci. Rev. 29, 2451–2461. http://dx.doi.org/10.1016/j.quascirev.2010.02.024.

Gutjahr, M., Frank, M., Lippold, J., Halliday, A.N., 2014. Peak Last Glacial weathering intensity on the North American continent recorded by the authigenic Hf isotope composition of North Atlantic deep-sea sediments. Quat. Sci. Rev. 99, 97–111. http://dx.doi.org/10.1016/j.quascirev.2014.06.022.

Haley, B.A., Frank, M., Spielhagen, R.F., Eisenhauer, A., 2008. Influence of brine formation on Arctic Ocean circulation over the past 15 million years. Nat. Geosci. 1, 68–72. http://dx.doi.org/10.1038/ngeo.2007.5.

Hathorne, E.C., Alard, O., James, R.H., Rogers, N.W., 2003. Determination of intratest variability of trace elements in foraminifera by laser ablation inductively coupled plasma-mass spectrometry. Geochem. Geophys. Geosyst. 4. http://dx.doi.org/10.1029/2003GC000539.

Hemming, S.R., 2004. Heinrich events: massive late Pleistocene detritus layers of the North Atlanitc and their global climate imprint. Rev. Geophys. 42. http://dx.doi.org/10.1029/2003RG000128.

Henrich, R., Baumann, K.-H., 1994. Evolution of the Norwegian Current and the Scandinavian Ice Sheets during the past 2.6 m.y.: evidence from ODP Leg 104 biogenic carbonate and terrigenous records. Palaeogeogr. Palaeoclimatol. Palaeoecol. 108, 75–94. http://dx.doi.org/10.1016/0031-0182(94)90023-X.

Hillaire-Marcel, C., de Vernal, A., McKay, J., 2011. Foraminifer isotope study of the Pleistocene Labrador Sea, northwest North Atlantic (IODP Sites 1302/03 and 1305), with emphasis on paleoceanographical differences between its "inner" and "outer" basins. Mar. Geol. 279, 188–198. http://dx.doi.org/10.1016/j.margeo.2010.11.001.

Hodell, D.A., Channell, J.E.T., Curtis, J.H., Romero, O.E., Röhl, U., 2008. Onset of "Hudson Strait" Heinrich events in the eastern North Atlantic at the end of the middle Pleistocene transition (~640 ka)? Paleoceanography 23, 1–16. http://dx.doi.org/10.1029/2008PA001591.

Jacobsen, S.B., Wasserburg, G.J., 1980. Sm-Nd isotopic evolution of chondrites. Earth Planet. Sci. Lett. 50, 139–155. http://dx.doi.org/10.1016/0012-821X(80)90125-9.

Jantschik, R., 1991. Mineralogische und geochemische Untersuchungen spätquartärer Tiefseesedimente aus dem Westeuropäischen Becken (bei 47° 30′N und 19° 30′W). Université de Neuchâtel.

Jeandel, C., 1993. Concentration and isotopic composition of Nd in the South Atlantic Ocean. Earth Planet. Sci. Lett. 117, 581–591. http://dx.doi.org/10.1016/0012-821X(93)90104-H.

Kempton, P.D., Fitton, J.G., Saunders, A.D., Nowell, G.M., Taylor, R.N., Hardarson, B.S., Pearson, G., 2000. The Iceland plume in space and time: a Sr-Nd-Pb-Hf study of the North Atlantic rifted margin. Earth Planet. Sci. Lett. 177, 255–271. http://dx.doi.org/10.1016/S0012-821X(00)00047-9.

Klevenz, V., Vance, D., Schmidt, D.N., Mezger, K., 2008. Neodymium isotopes in benthic foraminifera: core-top systematics and a down-core record from the Neogene South Atlantic. Earth Planet. Sci. Lett. 265, 571–587. http://dx.doi.org/10.1016/j.epsl.2007.10.053.

Koschinsky, A., Halbach, P., 1995. Sequential leaching of marine ferromanganese precipitates: genetic implications. Geochim. Cosmochim. Acta 59, 5113–5132. http://dx.doi.org/10.1016/0016-7037(95)00358-4.

Kraft, S., Frank, M., Hathorne, E.C., Weldeab, S., 2013. Assessment of seawater Nd isotope signatures extracted from foraminiferal shells and authigenic phases of Gulf of Guinea sediments. Geochim. Cosmochim. Acta 121, 414–435. http://dx.doi.org/10.1016/j.gca.2013.07.029.

Kuechler, R.R., Schefuß, E., Beckmann, B., Dupont, L., Wefer, G., 2013. NW African hydrology and vegetation during the Last Glacial cycle reflected in plant-wax-specific hydrogen and carbon isotopes. Quat. Sci. Rev. 82, 56–67. http://dx.doi.org/10.1016/j.quascirev.2013.10.013.

Kurzweil, F., Gutjahr, M., Vance, D., Keigwin, L., 2010. Authigenic Pb isotopes from the Laurentian Fan: changes in chemical weathering and patterns of North American freshwater runoff during the last deglaciation. Earth Planet. Sci. Lett. 299, 458–465. http://dx.doi.org/10.1016/j.epsl.2010.09.031.

Lacan, F., Jeandel, C., 2004a. Denmark Strait water circulation traced by heterogeneity in neodymium isotopic compositions. Deep-Sea Res. I Oceanogr. Res. Pap. 51, 71–82. http://dx.doi.org/10.1016/j.dsr.2003.09.006.

Lacan, F., Jeandel, C., 2004b. Neodymium isotopic composition and rare earth element concentrations in the deep and intermediate Nordic Seas: constraints on the Iceland Scotland Overflow Water signature. Geochem. Geophys. Geosyst. 5, Q11006. http://dx.doi.org/10.1029/2004GC000742.

Lacan, F., Jeandel, C., 2005a. Neodymium isotopes as a new tool for quantifying exchange fluxes at the continent-ocean interface. Earth Planet. Sci. Lett. 232, 245–257. http://dx.doi.org/10.1016/j.epsl.2005.01.004.

Lacan, F., Jeandel, C., 2005b. Acquisition of the neodymium isotopic composition of the North Atlantic Deep Water. Geochem. Geophys. Geosyst. 6, Q12008. http://dx.doi.org/10.1029/2005GC000956.

Lacan, F., Tachikawa, K., Jeandel, C., 2012. Neodymium isotopic composition of the oceans: a compilation of seawater data. Chem. Geol. 300-301, 177–184. http://dx.doi.org/10.1016/j.chemgeo.2012.01.019.

Lambelet, M., van de Flierdt, T., Crocket, K., Rehkämper, M., Kreissig, K., Coles, B., Rijkenberg, M.J.A., Gerringa, L.J.A., de Baar, H.J.W., Steinfeldt, R., 2016. Neodymium isotopic composition and concentration in the western North Atlantic Ocean: results from the GEOTRACES GA02 section. Geochim. Cosmochim. Acta 177, 1–29. http://dx.doi.org/10.1016/j.gca.2015.12.019.

Lippold, J., Gutjahr, M., Blaser, P., Christner, E., Ferreira, M.L.d.C., Mulitza, S., Christl, M., Wombacher, F., Böhm, E., Antz, B., Cartapanis, O., Vogel, H., Jaccard, S.L., 2016. Deep water provenience and dynamics of the (de)glacial Atlantic meridional overturning circulation. Earth Planet. Sci. Lett. 445, 68–78. http://dx.doi.org/10.1016/j.epsl.2016.04.013.

Martin, E.E., Scher, H.D., 2004. Preservation of seawater Sr and Nd isotopes in fossil fish teeth: bad news and good news. Earth Planet. Sci. Lett. 220, 25–39. http://dx.doi.org/10.1016/S0012-821X(04)00030-5.

Martin, E.E., Blair, S.W., Kamenov, G.D., Scher, H.D., Bourbon, E., Basak, C., Newkirk, D.N., 2010. Extraction of Nd isotopes from bulk deep sea sediments for paleoceanographic studies on Cenozoic time scales. Chem. Geol. 269, 414–431. http://dx.doi.org/10.1016/j.chemgeo.2009.10.016.

Martínez-Botí, M.A., Vance, D., Mortyn, P.G., 2009. Nd/Ca ratios in plankton-towed and core top foraminifera: confirmation of the water column acquisition of Nd. Geochem. Geophys. Geosyst. 10, Q08018. http://dx.doi.org/10.1029/2009GC002701.

Molina-Kescher, M., Frank, M., Hathorne, E., 2014a. South Pacific dissolved Nd isotope compositions and rare earth element distributions: water mass mixing versus biogeochemical cycling. Geochim. Cosmochim. Acta 127, 171–189. http://dx.doi.org/10.1016/j.gca.2013.11.038.

Molina-Kescher, M., Frank, M., Hathorne, E.C., 2014b. Nd and Sr isotope compositions of different phases of surface sediments in the South Pacific: extraction of seawater signatures, boundary exchange, and detrital/dust provenance. Geochem. Geophys. Geosyst. 15, 3502–3520. http://dx.doi.org/10.1002/2014GC005443.

Nance, W., Taylor, S., 1976. Rare earth element patterns and crustal evolution—I. Australian post-Archean sedimentary rocks. Geochim. Cosmochim. Acta 40, 1539–1551. http://dx.doi.org/10.1016/0016-7037(76)90093-4.

Nürnberg, D., Bijma, J., Hemleben, C., 1996. Assessing the reliability of magnesium in foraminiferal calcite as a proxy for water mass temperatures. Geochim. Cosmochim. Acta 60, 803–814. http://dx.doi.org/10.1016/0016-7037(95)00446-7.

Öhlander, B., Ingri, J., Land, M., Schöberg, H., 2000. Change of Sm-Nd isotope composition during weathering of till. Geochim. Cosmochim. Acta 64, 813–820. http://dx.doi.org/10.1016/S0016-7037(99)00365-8.

Pahnke, K., Goldstein, S., Hemming, S., 2008. Abrupt changes in Antarctic Intermediate Water circulation over the past 25,000 years. Nat. Geosci. 1, 870–874. http://dx.doi.org/10.1038/ngeo360.

Palmer, M., 1985. Rare earth elements in foraminifera tests. Earth Planet. Sci. Lett. 73, 285–298. http://dx.doi.org/10.1016/0012-821X(85)90077-9.

Pena, L.D., Calvo, E., Cacho, I., Eggins, S., Pelejero, C., 2005. Identification and removal of Mn-Mg-rich contaminant phases on foraminiferal tests: implications for Mg/Ca past temperature reconstructions. Geochem. Geophys. Geosyst. 6. http://dx.doi.org/10.1029/2005GC000930.

Piepgras, D.J., Wasserburg, G.J., 1980. Neodymium isotopic variations in seawater. Earth Planet. Sci. Lett. 50, 128–138. http://dx.doi.org/10.1016/0012-821X(80)90124-7.

Piepgras, D.J., Wasserburg, G.J., 1983. Influence of the Mediterranean outflow on the isotopic composition of neodymium in waters of the North Atlantic. J. Geophys. Res. 88, 5997–6006.

Piepgras, D.J., Wasserburg, G.J., Dasch, E.J., 1979. The isotopic composition of Nd in different ocean masses. Earth Planet. Sci. Lett. 45, 223–236. http://dx.doi.org/10.1016/0012-821X(79)90125-0.

Pin, C., Briot, D., Bassin, C., Poitrasson, F., 1994. Concomitant separation of strontium and samarium-neodymium for isotopic analysis in silicate samples, based on specific extraction chromatography. Anal. Chim. Acta 298, 209–217. http://dx.doi.org/10.1016/0003-2670(94)00274-6.

Piotrowski, A.M., Goldstein, S.L., Hemming, S.R., Fairbanks, R.G., 2004. Intensification and variability of ocean thermohaline circulation through the last deglaciation. Earth Planet. Sci. Lett. 225, 205–220. http://dx.doi.org/10.1016/j.epsl.2004.06.002.

Piotrowski, A.M., Goldstein, S.L., Hemming, S.R., Fairbanks, R.G., Zylberberg, D.R., 2008. Oscillating glacial northern and southern deep water formation from combined neodymium and carbon isotopes. Earth Planet. Sci. Lett. 272, 394–405. http://dx.doi.org/10.1016/j.epsl.2008.05.011.

Piotrowski, A.M., Galy, A., Nicholl, J.A.L., Roberts, N., Wilson, D.J., Clegg, J.A., Yu, J., 2012. Reconstructing deglacial North and South Atlantic deep water sourcing using foraminiferal Nd isotopes. Earth Planet. Sci. Lett. 357-358, 289–297. http://dx.doi.org/10.1016/j.epsl.2012.09.036.

Poulton, S., Canfield, D., 2005. Development of a sequential extraction procedure for iron: implications for iron partitioning in continentally derived particulates. Chem. Geol. 214, 209–221. http://dx.doi.org/10.1016/j.chemgeo.2004.09.003.

Poulton, S.W., Krom, M.D., Raiswell, R., 2004. A revised scheme for the reactivity of iron (oxyhydr)oxide minerals towards dissolved sulfide. Geochim. Cosmochim. Acta 68, 3703–3715. http://dx.doi.org/10.1016/j.gca.2004.03.012.

Rempfer, J., Stocker, T.F., Joos, F., Dutay, J.C., Siddall, M., 2011. Modelling Nd-isotopes with a coarse resolution ocean circulation model: sensitivities to model parameters and source/sink distributions. Geochim. Cosmochim. Acta 75, 5927–5950. http://dx.doi.org/10.1016/j.gca.2011.07.044.

Rickli, J., Gutjahr, M., Vance, D., Fischer-Gödde, M., Hillenbrand, C.-D., Kuhn, G., 2014. Neodymium and hafnium boundary contributions to seawater along the West Antarctic continental margin. Earth Planet. Sci. Lett. 394, 99–110. http://dx.doi.org/10.1016/j.epsl.2014.03.008.

Roberts, N.L., Piotrowski, A.M., 2015. Radiogenic Nd isotope labeling of the northern NE Atlantic during MIS 2. Earth Planet. Sci. Lett. 423, 125–133. http://dx.doi.org/10.1016/j.epsl.2015.05.011.

Roberts, N.L., Piotrowski, A.M., McManus, J.F., Keigwin, L.D., 2010. Synchronous deglacial overturning and water mass source changes. Science 327, 75–78. http://dx.doi.org/10.1126/science.1178068.

Roberts, N.L., Piotrowski, A.M., Elderfield, H., Eglinton, T.I., Lomas, M.W., 2012. Rare earth element association with foraminifera. Geochim. Cosmochim. Acta 94, 57–71. http://dx.doi.org/10.1016/j.gca.2012.07.009.

Robinson, L.F., Adkins, J.F., Frank, N., Gagnon, A.C., Prouty, N.G., Brendan Roark, E., de Flierdt, T.v., 2014. The geochemistry of deep-sea coral skeletons: a review of vital effects and applications for palaeoceanography. Deep-Sea Res. II Top. Stud. Oceanogr. 99, 184–198. http://dx.doi.org/10.1016/j.dsr2.2013.06.005.

Rousseau, T.C.C., Sonke, J.E., Chmeleff, J., van Beek, P., Souhaut, M., Boaventura, G., Seyler, P., Jeandel, C., 2015. Rapid neodymium release to marine waters from lithogenic sediments in the Amazon estuary. Nat. Commun. 6, 7592. http://dx.doi.org/10.1038/ncomms8592.

Rutberg, R., Hemming, S., Goldstein, S., 2000. Reduced North Atlantic Deep Water flux to the glacial Southern Ocean inferred from neodymium isotope ratios. Nature 405, 935–938. http://dx.doi.org/10.1038/35016049.

Sinha, S.P., 1982. Systematics and the properties of the lanthanides. Polyhedron http://dx.doi.org/10.1016/S0277-5387(00)81087-6.

Skinner, L.C., Scrivner, A.E., Vance, D., Barker, S., Fallon, S., Waelbroeck, C., 2013. North Atlantic versus southern ocean contributions to a deglacial surge in deep ocean ventilation. Geology 41, 667–670. http://dx.doi.org/10.1130/G34133.1.

Staudigel, H., Doyle, P., Zindler, A., 1985. Sr and Nd isotope systematics in fish teeth. Earth Planet. Sci. Lett. 76, 45–56. http://dx.doi.org/10.1016/0012-821X(85)90147-5.

Stein, R., Hefter, J., Grützner, J., Voelker, A., Naafs, B.D.A., 2009. Variability of surface water characteristics and Heinrich-like events in the Pleistocene midlatitude North Atlantic Ocean: Biomarker and XRD records from IODP Site U1313 (MIS 16–9). Paleoceanography 24, PA2203. http://dx.doi.org/10.1029/2008pa001639.

Stichel, T., Hartman, A.E., Duggan, B., Goldstein, S.L., Scher, H., Pahnke, K., 2015. Separating biogeochemical cycling of neodymium from water mass mixing in the Eastern North Atlantic. Earth Planet. Sci. Lett. 412, 245–260. http://dx.doi.org/10.1016/j.epsl.2014.12.008.

Tachikawa, K., Jeandel, C., Roy-Barman, M., 1999. A new approach to the Nd residence time in the ocean: the role of atmospheric inputs. Earth Planet. Sci. Lett. 170, 433–446. http://dx.doi.org/10.1016/S0012-821X(99)00127-2.

Tachikawa, K., Athias, V., Jeandel, C., 2003. Neodymium budget in the modern ocean and paleo-oceanographic implications. J. Geophys. Res. 108, 3254. http://dx.doi.org/10.1029/1999JC000285.

Tachikawa, K., Toyofuku, T., Basile-Doelsch, I., Delhaye, T., 2013. Microscale neodymium distribution in sedimentary planktonic foraminiferal tests and associated mineral phases. Geochim. Cosmochim. Acta 100, 11–23. http://dx.doi.org/10.1016/j.gca.2012.10.010.

Tachikawa, K., Piotrowski, A.M., Bayon, G., 2014. Neodymium associated with foraminiferal carbonate as a recorder of seawater isotopic signatures. Quat. Sci. Rev. 88, 1–13. http://dx.doi.org/10.1016/j.quascirev.2013.12.027.

Takematsu, N., Sato, Y., Okabe, S., 1989. Factors controlling the chemical composition of marine manganese nodules and crusts: a review and synthesis. Mar. Chem. 26, 41–56.

Takeno, N., 2005. Atlas of Eh-pH diagrams. Geol. Surv. Japan Open File Rep.

Tanaka, T., Togashi, S., Kamioka, H., Amakawa, H., Kagami, H., Hamamoto, T., Yuhara, M., Orihashi, Y., Yoneda, S., Shimizu, H., Kunimaru, T., Takahashi, K., Yanagi, T., Nakano, T., Fujimaki, H., Shinjo, R., Asahara, Y., Tanimizu, M., Dragusanu, C., 2000. JNdi-1: A neodymium isotopic reference in consistency with LaJolla neodymium. Chem. Geol. 168, 279–281. http://dx.doi.org/10.1016/S0009-2541(00)00198-4.

Tessier, A., Campbell, P.G.C., Bisson, M., 1979. Sequential extraction procedure for the speciation of particulate trace metals. Anal. Chem. 51, 844–851. http://dx.doi.org/10.1021/ac50043a017.

van de Flierdt, T., Frank, M., 2010. Neodymium isotopes in paleoceanography. Quat. Sci. Rev. 29, 2439–2441. http://dx.doi.org/10.1016/j.quascirev.2010.07.001.

van de Flierdt, T., Robinson, L.F., Adkins, J.F., Hemming, S.R., Goldstein, S.L., 2006. Temporal stability of the neodymium isotope signature of the Holocene to glacial North Atlantic. Paleoceanography 21. http://dx.doi.org/10.1029/2006pa001294.

Vance, D., Burton, K., 1999. Neodymium isotopes in planktonic foraminifera: a record of the response of continental weathering and ocean circulation rates to climate change. Earth Planet. Sci. Lett. 173, 365–379. http://dx.doi.org/10.1016/S0012-821X(99)00244-7.

Vance, D., Scrivner, A.E., Beney, P., 2004. The use of foraminifera as a record of the past neodymium isotope composition of seawater. Paleoceanography 19, PA2009. http://dx.doi.org/10.1029/2003PA000957.

Vance, D., Teagle, D.a.H., Foster, G.L., 2009. Variable Quaternary chemical weathering fluxes and imbalances in marine geochemical budgets. Nature 458, 493–496. http://dx.doi.org/10.1038/nature07828.

von Blanckenburg, F., Nägler, T., 2001. Weathering versus circulation-controlled changes in radiogenic isotope tracer composition of the Labrador Sea and North Atlantic Deep Water. Paleoceanography 16, 424–434. http://dx.doi.org/10.1029/2000PA000550.

Weill, D.F., Drake, M.J., 1973. Europium anomaly in plagioclase feldspar: experimental results and semiquantitative model. Science 180, 1059–1060. http://dx.doi.org/10.1126/science.180.4090.1059.

Wilson, D.J., Piotrowski, A.M., Galy, A., McCave, I.N., 2012. A boundary exchange influence on deglacial neodymium isotope records from the deep western Indian Ocean. Earth Planet. Sci. Lett. 341-344, 35–47. http://dx.doi.org/10.1016/j.epsl.2012.06.009.

Wilson, D.J., Piotrowski, A.M., Galy, A., Clegg, J.A., 2013. Reactivity of neodymium carriers in deep sea sediments: implications for boundary exchange and paleoceanography. Geochim. Cosmochim. Acta 109, 197–221. http://dx.doi.org/10.1016/j.gca.2013.01.042.

Wilson, D.J., Crocket, K.C., Van De Flierdt, T., Robinson, L.F., Adkins, J.F., 2014. Dynamic intermediate ocean circulation in the North Atlantic during Heinrich Stadial 1: a radiocarbon and neodymium isotope perspective. Paleoceanography 29, 1072–1093. http://dx.doi.org/10.1002/2014PA002674.

Wilson, D.J., Piotrowski, A.M., Galy, A., Banakar, V.K., 2015. Interhemispheric controls on deep ocean circulation and carbon chemistry during the last two glacial cycles. Paleoceanography 30, 621–641. http://dx.doi.org/10.1002/2014PA002707.

Yokoyama, T., Makishima, A., Nakamura, E., 1999. Evaluation of the coprecipitation of incompatible trace elements with fluoride during silicate rock dissolution by acid digestion. Chem. Geol. 157, 175–187. http://dx.doi.org/10.1016/S0009-2541(98)00206-X.

Zheng, X.Y., Plancherel, Y., Saito, M.A., Scott, P.M., Henderson, G.M., 2016. Rare earth elements (REEs) in the tropical South Atlantic and quantitative deconvolution of their non-conservative behavior. Geochim. Cosmochim. Acta 177, 217–237. http://dx.doi.org/10.1016/j.gca.2016.01.018.